Superconducting circuits for quantum technologies

Yasunobu Nakamura

RIKEN Center for Quantum Computing

Department of Applied Physics, Graduate School of Engineering,
The University of Tokyo

APPLIED PHYSICS
THE UNIVERSITY OF TOKYO

RIKEN

RIKEN QUANTUM COMPUTING

RIKEN Center for Quantum Computing (RQC)

since April 2021

RIKEN QUANTUM COMPUTING

RQC PIs


Bartosz Regula


Hayato Goto


Seigo Tarucha


Tomotaka Kuwahara


Eisuke Abe


JawShen Tsai


Akira Furusawa


Shintaro Sato


Erika Kawakami


Yasunobu Nakamura


Shinichi Yorozu


Yutaka Tabuchi


Daniel Loss


Atsushi Noguchi


Takeshi Fukuhara


Seiji Yunoki


Franco Nori


Keisuke Fujii

RQC research topics

Superconducting quantum computers

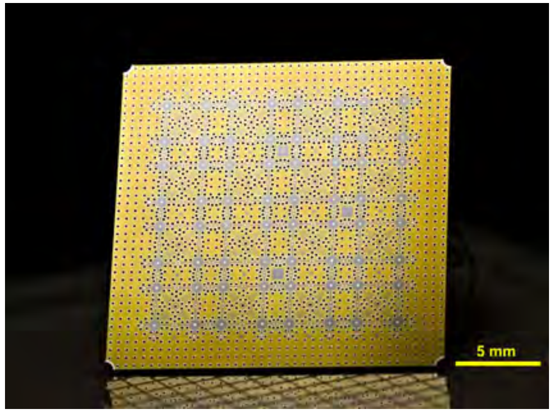

Optical quantum computers

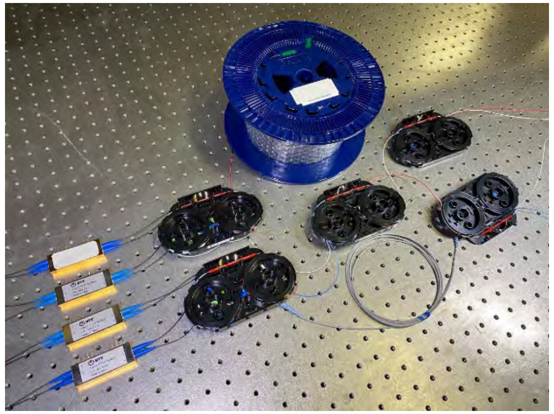

Silicon quantum computers

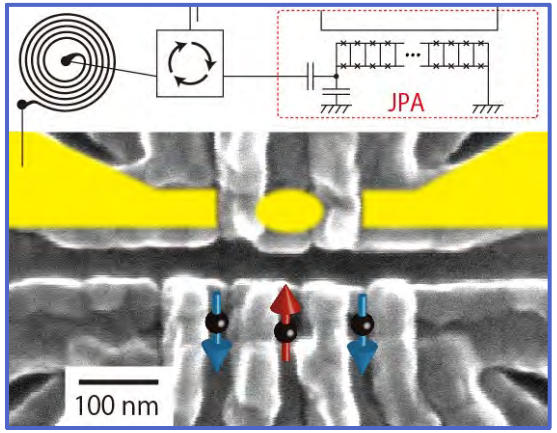

Other quantum platforms

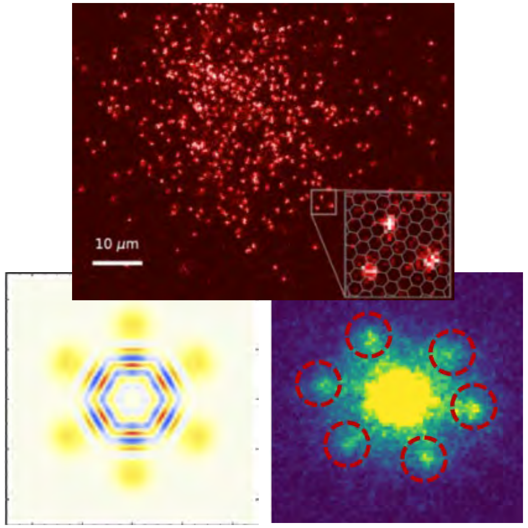

Quantum computing theory

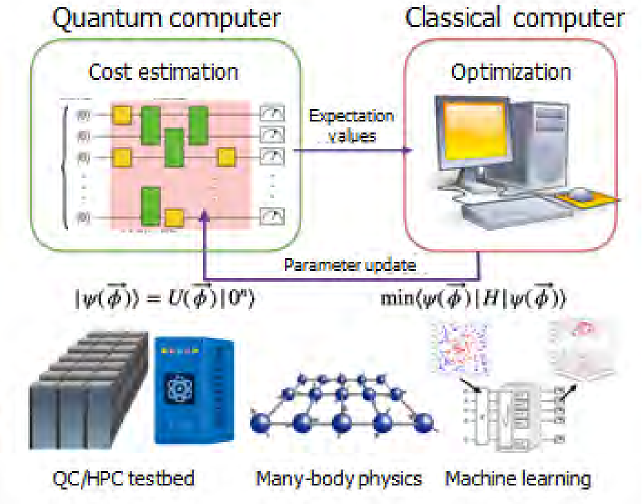

20th century: Century of quantum mechanics

1900 Blackbody radiation (Planck)
1905 Photoelectric effect (Einstein)
1913 Bohr model of atoms

1925 Matrix mechanics (Heisenberg)
1925 Wave mechanics (Schrödinger)

1928 Band theory in solids (Bloch)

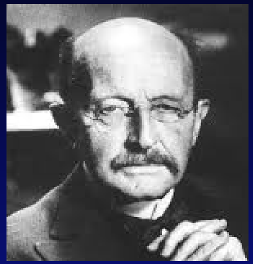
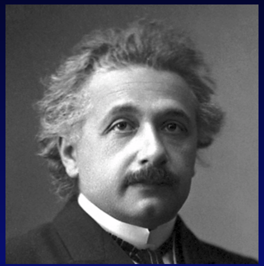
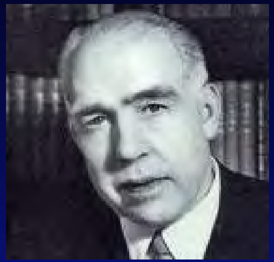



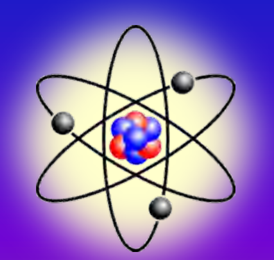

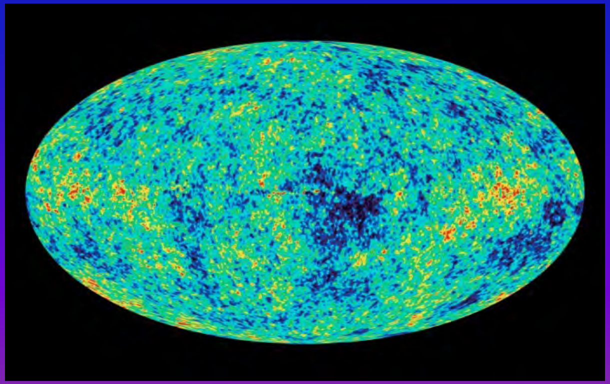

Moore’s law 1965～

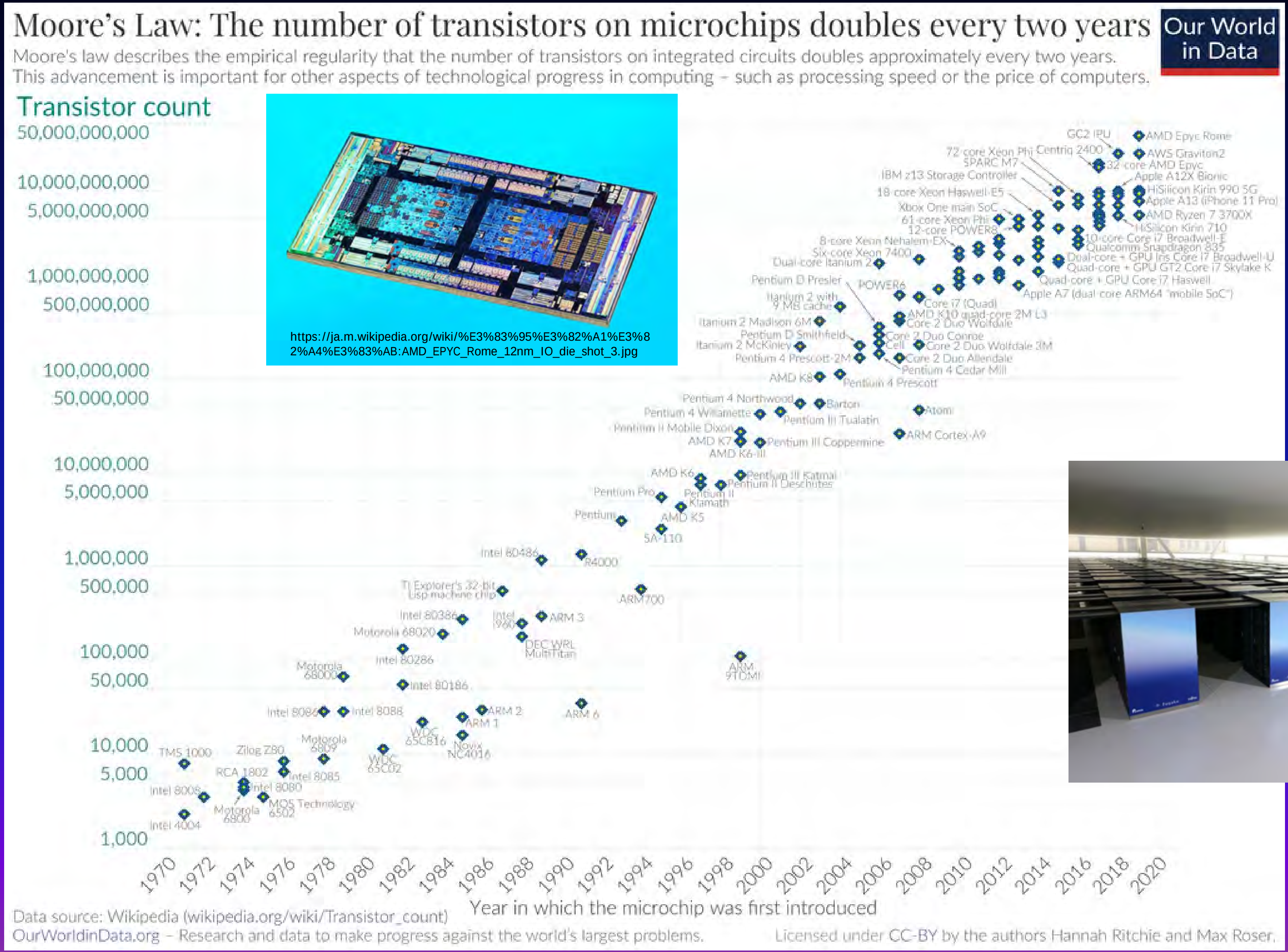

Fugaku@RIKEN

20^{th} century: Century of Quantum Mechanics
21^{st} century: Century of Quantum Information Science

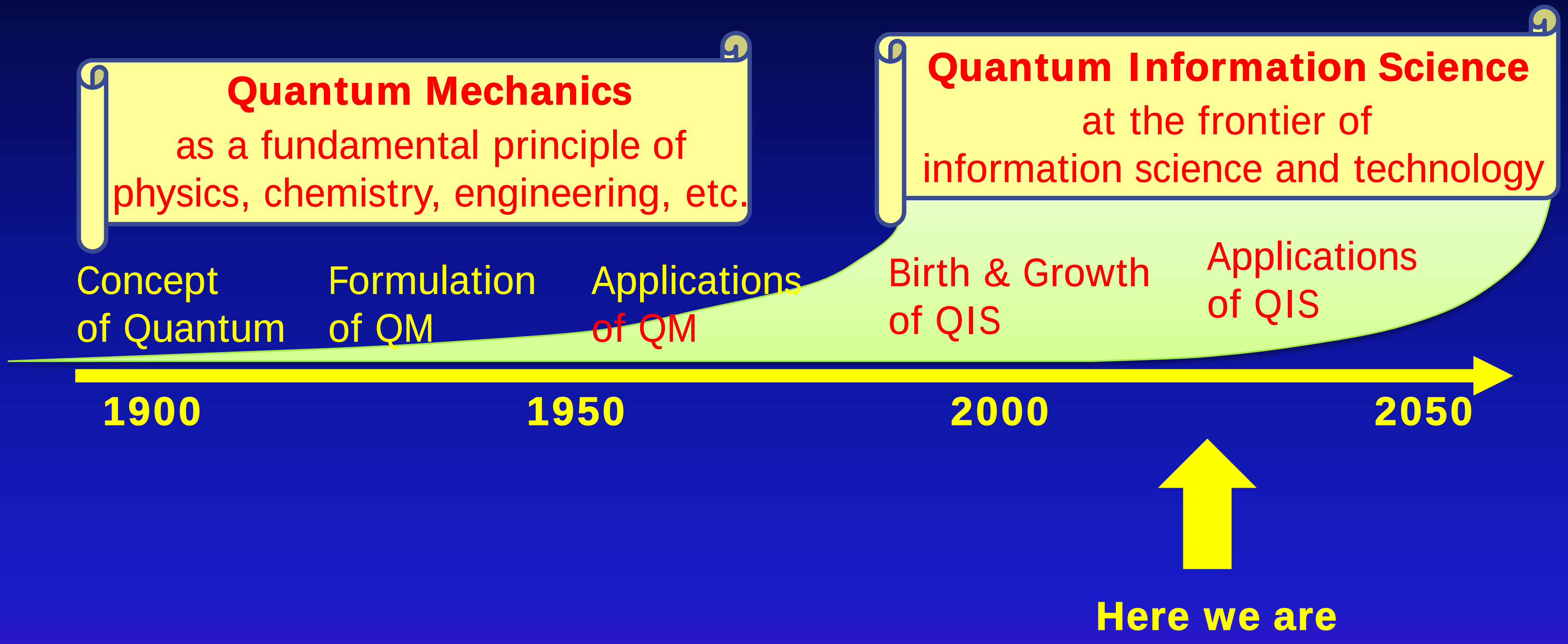

Our challenge:

How far can we control quantum systems in terms of the number of degrees of freedom, time, speed, precision, etc.?

Schrödinger's paradox

Macro-realism vs. Quantum mechanics

Schrödinger 1935

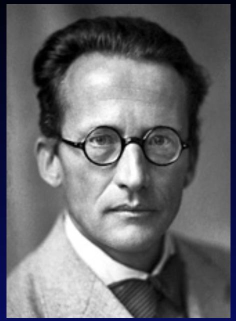

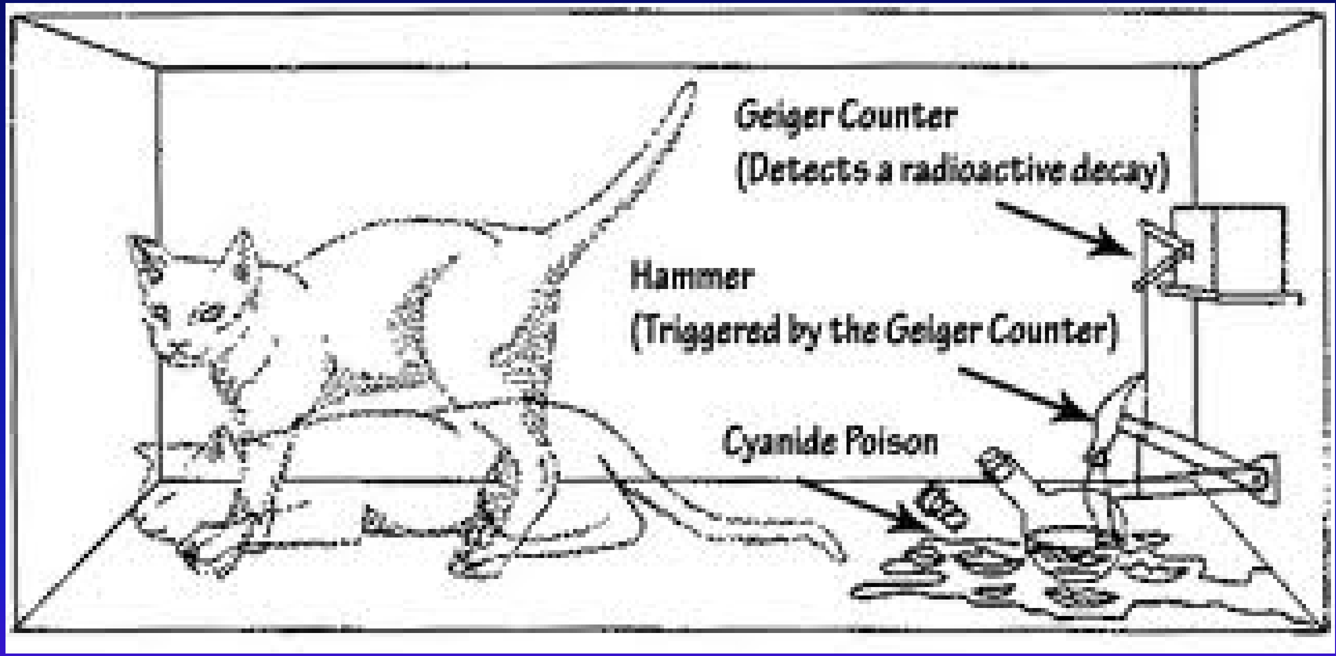

Dead and Alive

Macroscopic quantum coherence

Leggett 1980

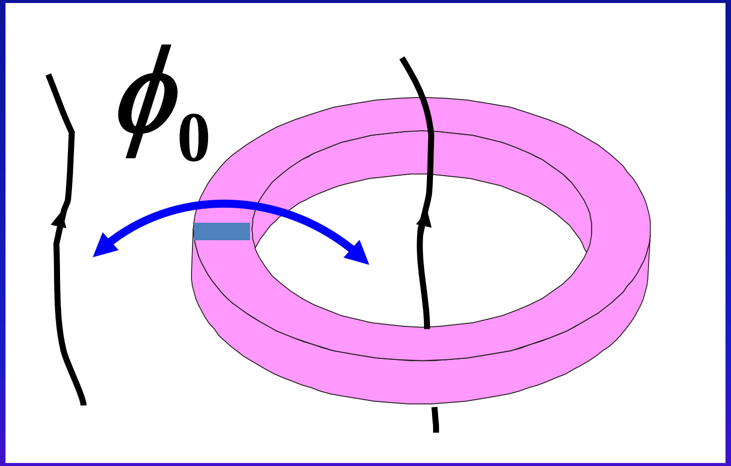

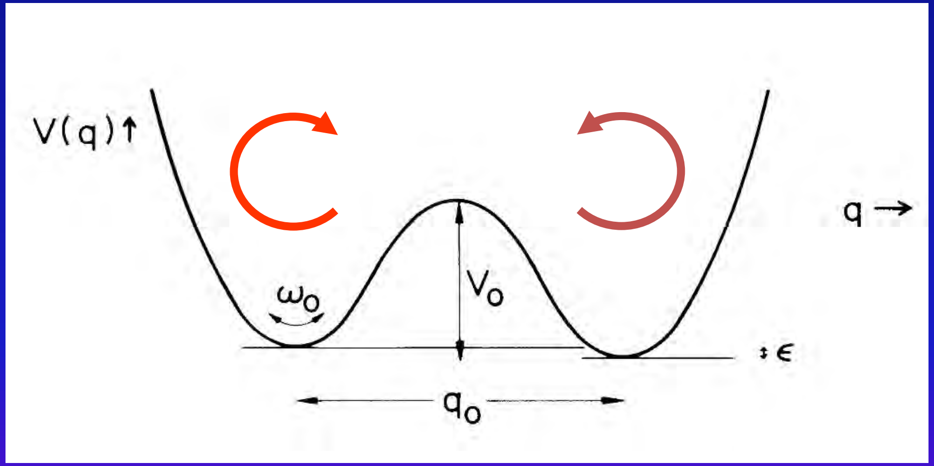

Superconducting loop
with a Josephson junction

Josephson effect

B. D. Josephson 1962

Number $n \Leftrightarrow$ Phase θ

$$[n, \theta] = -i$$

Cooper-pair tunneling
-2e

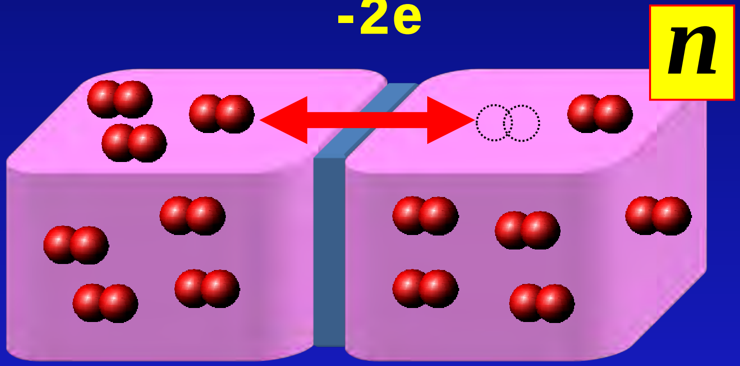

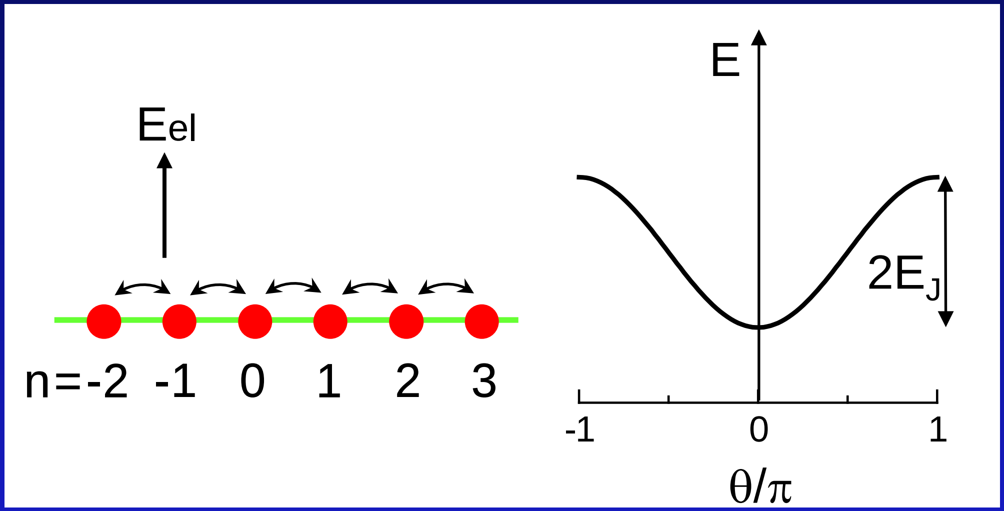

$$H = -\frac{E_J}{2} \sum_n \{|n\rangle\langle n+1| + |n+1\rangle\langle n|\} = -\int_0^{2\pi} d\theta E_J \cos\theta |\theta\rangle\langle\theta|$$

1D tight-binding model $\Rightarrow$ Bloch band

$$|\theta\rangle = \sum_n e^{in\theta} |n\rangle$$

Macroscopic quantum tunneling

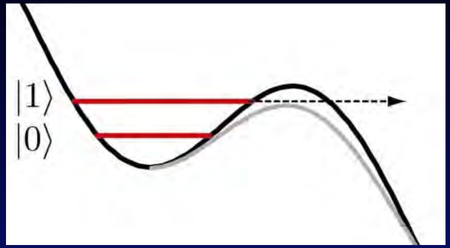

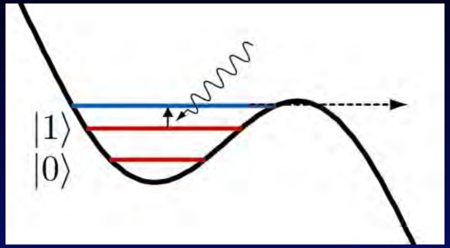

Saturation of escape rate

Energy level quantization

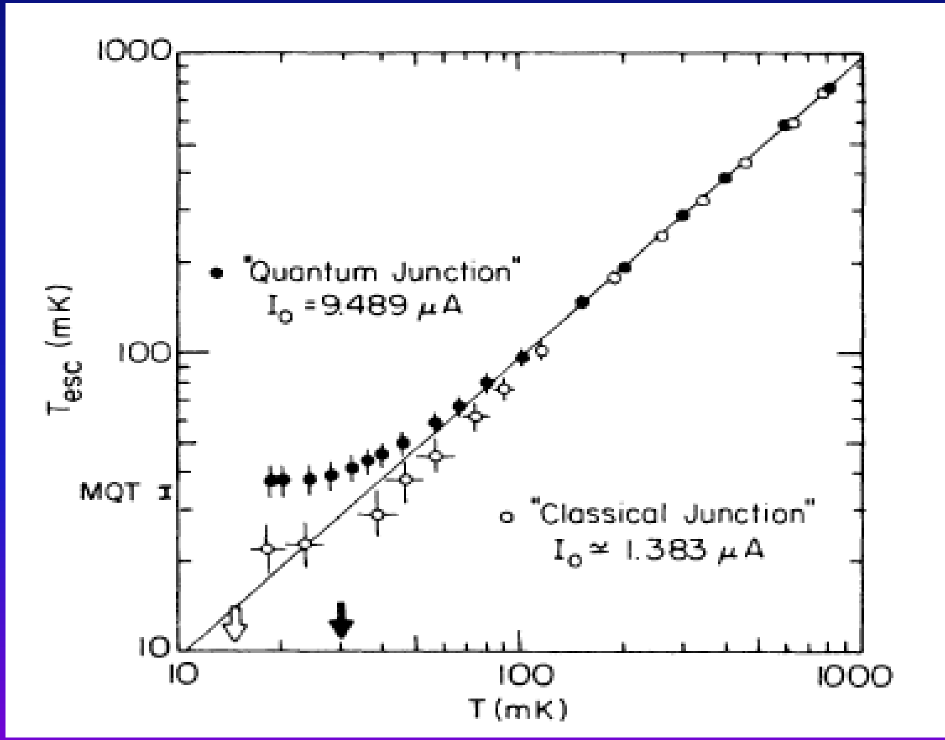

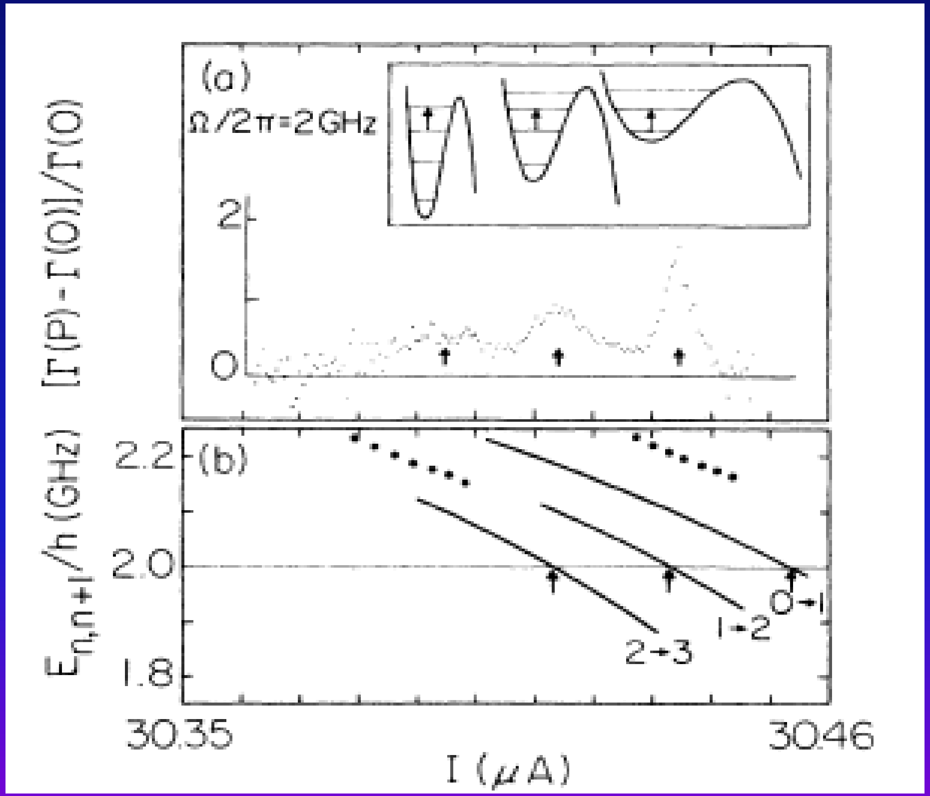

J. M. Martinis, M. H. Devoret, et al. PRB 35, 4682 (1987).
R.F. Voss and R.A. Webb (IBM), PRL 47, 265 (1981); D.B. Schwarz et al. (SUNY), PRL 55, 1547 (1985).

Single-electron devices

1990s

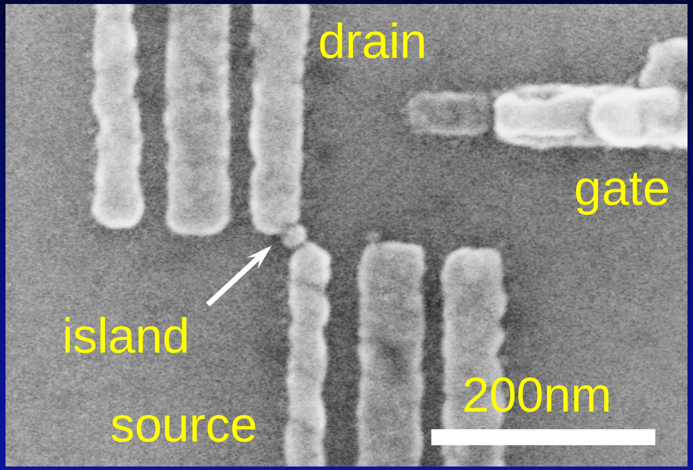

$$E_C \equiv \frac{e^2}{2C_\Sigma} \sim 11.5\,\mathrm{meV}$$

$$E_C/k_B \sim 130\,\mathrm{K}$$

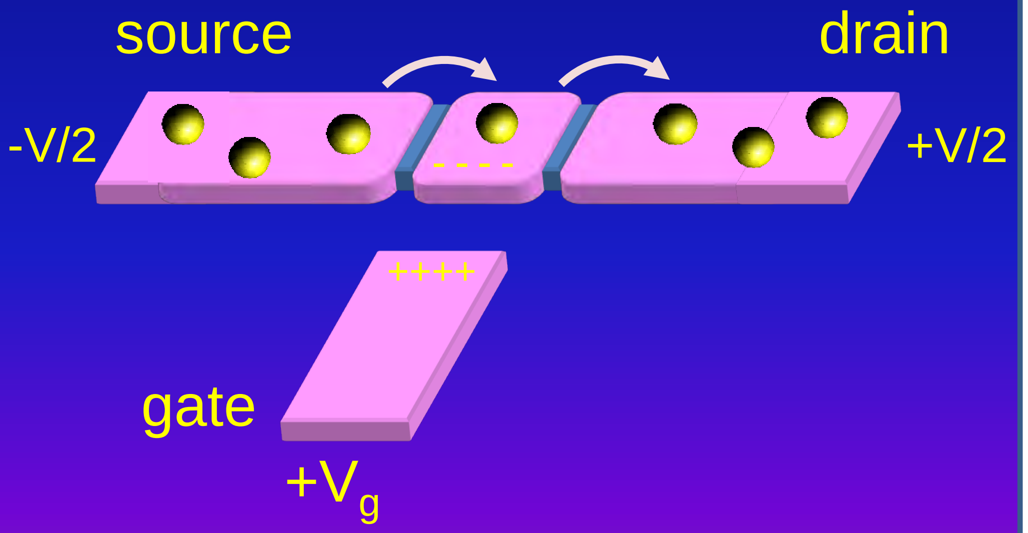

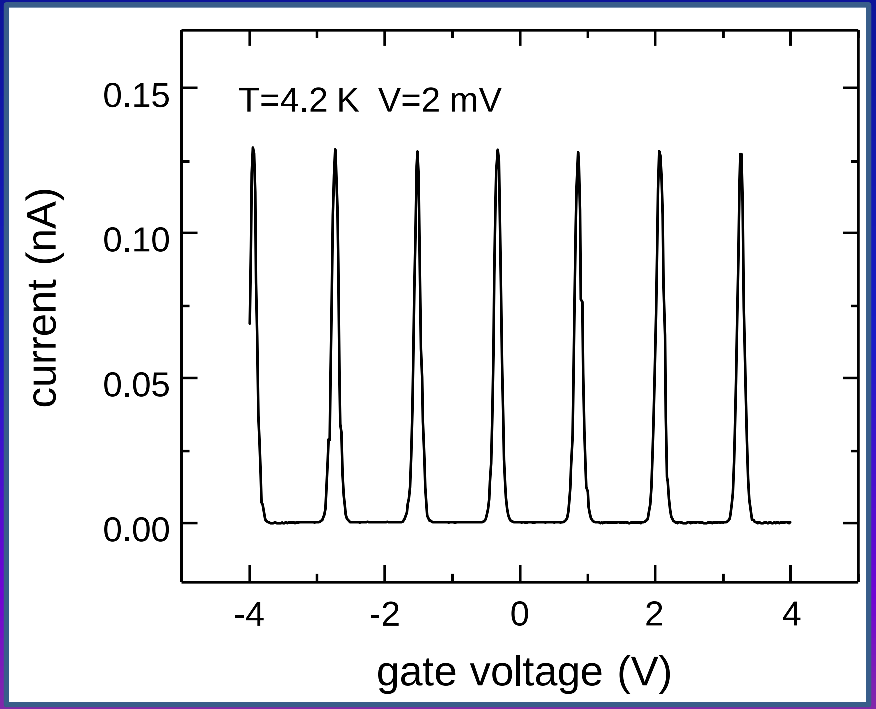

Superposition of charge-number states in Cooper-pair box

Spectroscopy of Energy-Level Splitting between Two Macroscopic Quantum States of Charge Coherently Superposed by Josephson Coupling

Y. Nakamura, C. D. Chen, and J. S. Tsai
NEC Fundamental Research Laboratories, Tsukuba, Ibaraki 305, Japan
(Received 16 April 1997)

PRL 1997

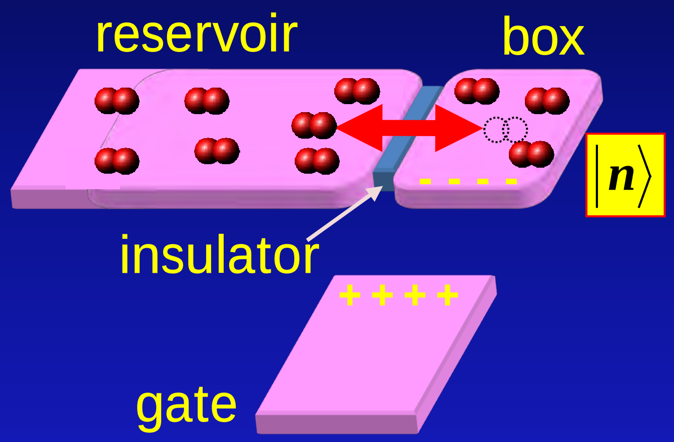

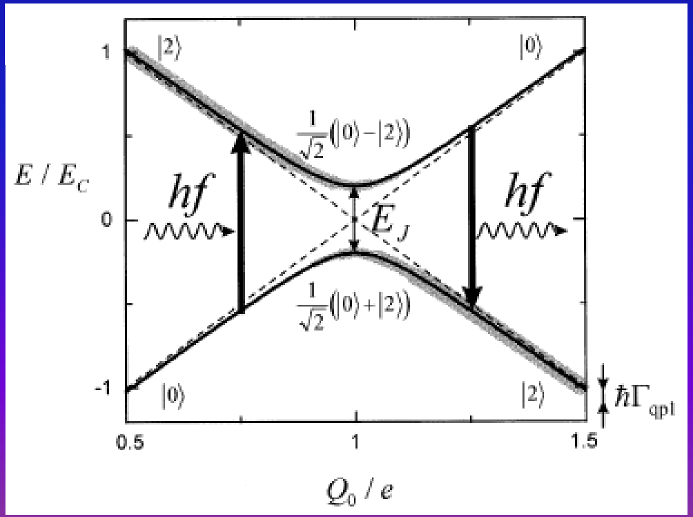

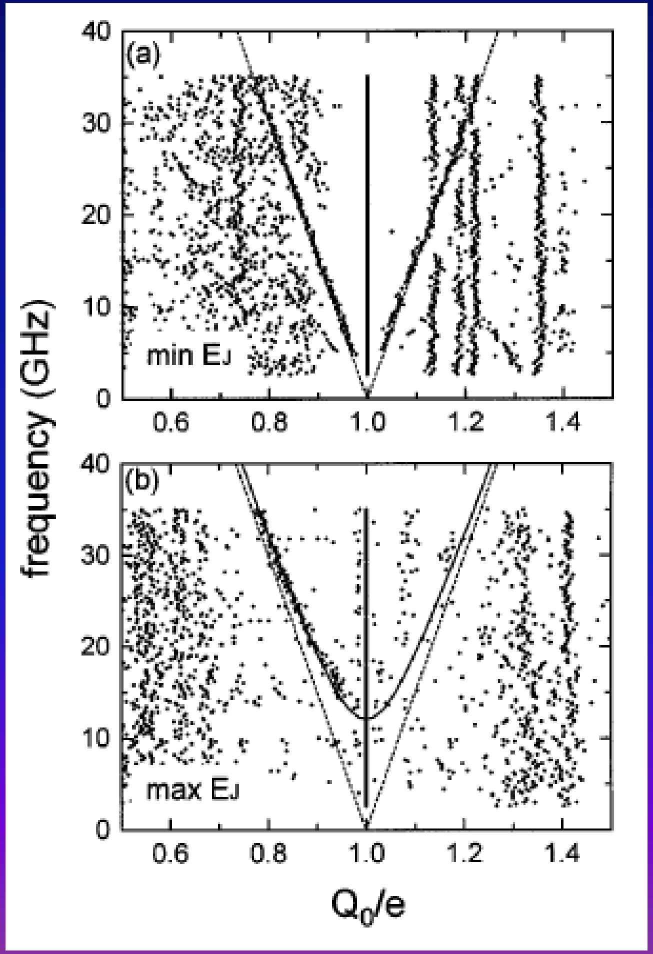

Superposition of charge-number states in Cooper-pair box

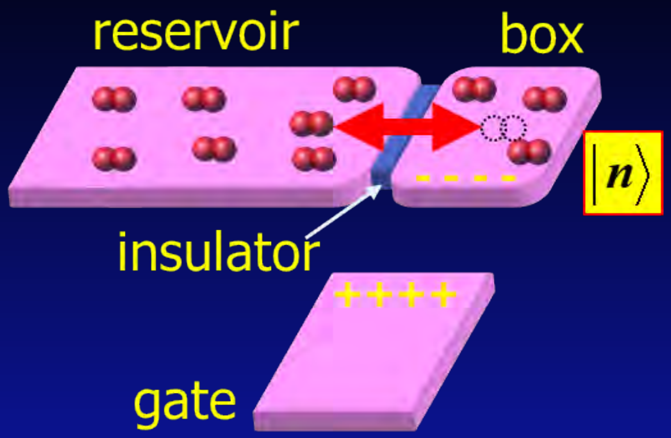

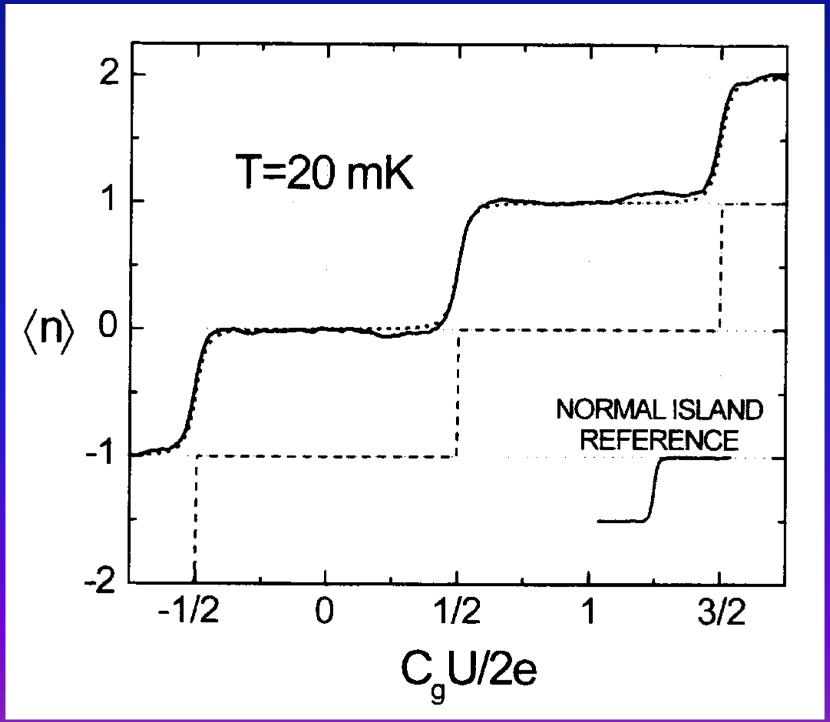

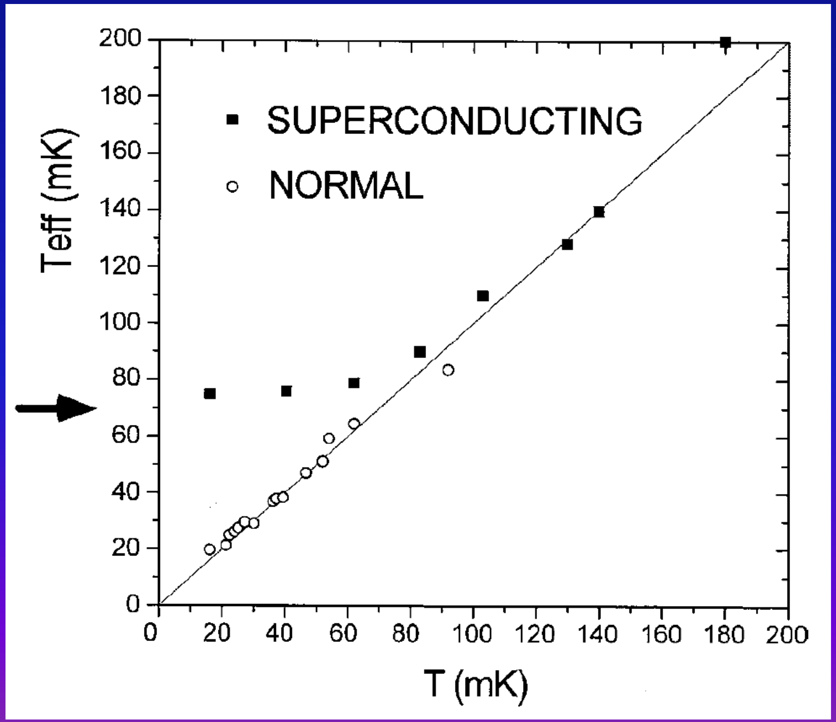

V. Bouchiat et al. Phys. Scr. T76, 165 (1998) Saclay

Superconducting quantum bits

Charge qubit

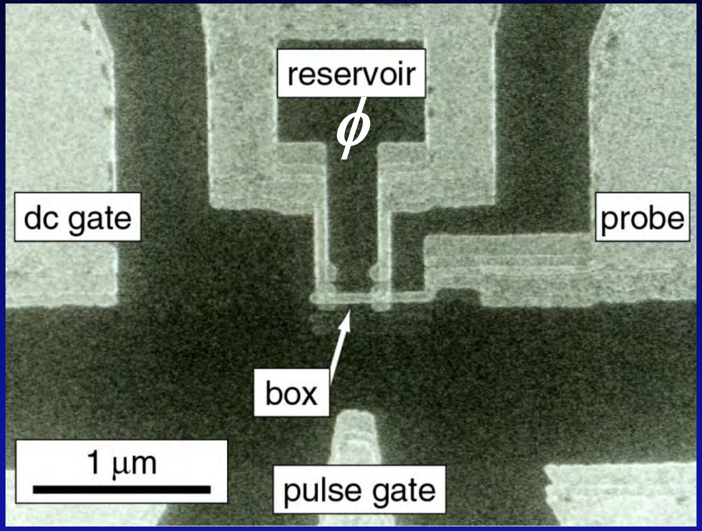

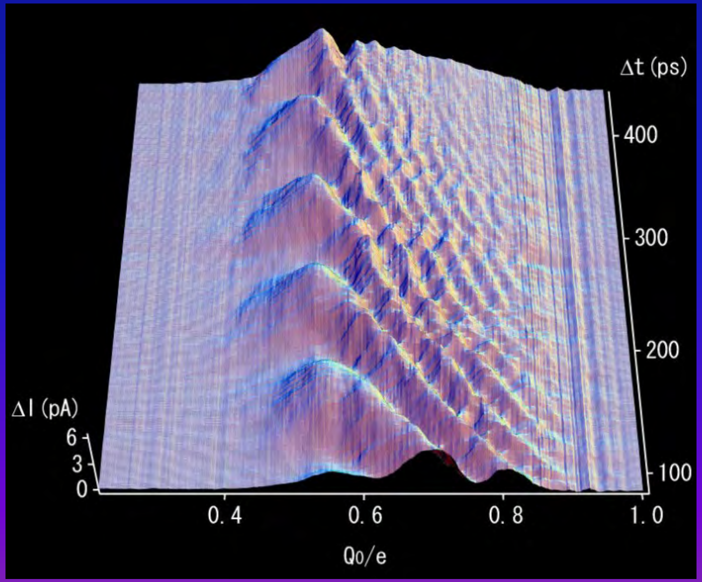

YN, Pashkin, Tsai, Nature (1999)

Flux qubit

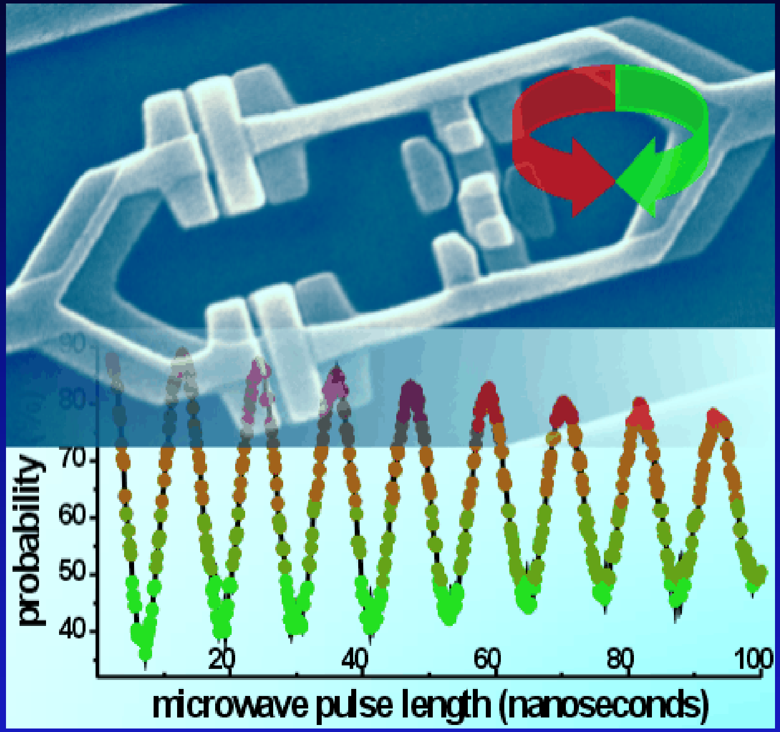

Chiorescu, YN, Harmans, Mooij, Science (2003)

Artificial two-level system in circuits

Coherent control of macroscopic system

Superconducting qubit – nonlinear resonator

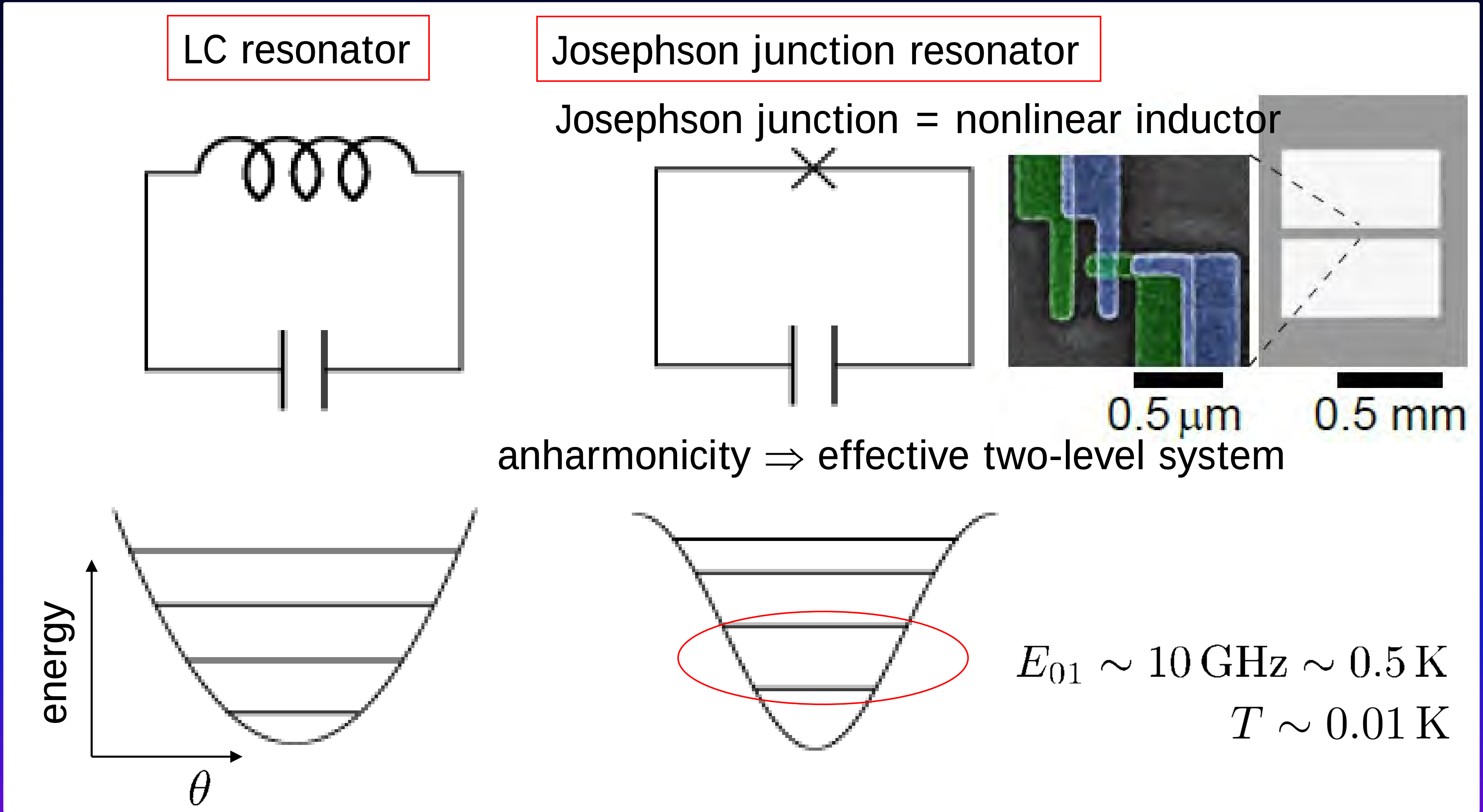

inductive energy = confinement potential
charging energy = kinetic energy ⇒ quantized states

Superconducting qubit – nonlinear resonator

LC resonator | **Superconducting qubit** | **Atom**

= Artificial atom

~mm

~Å

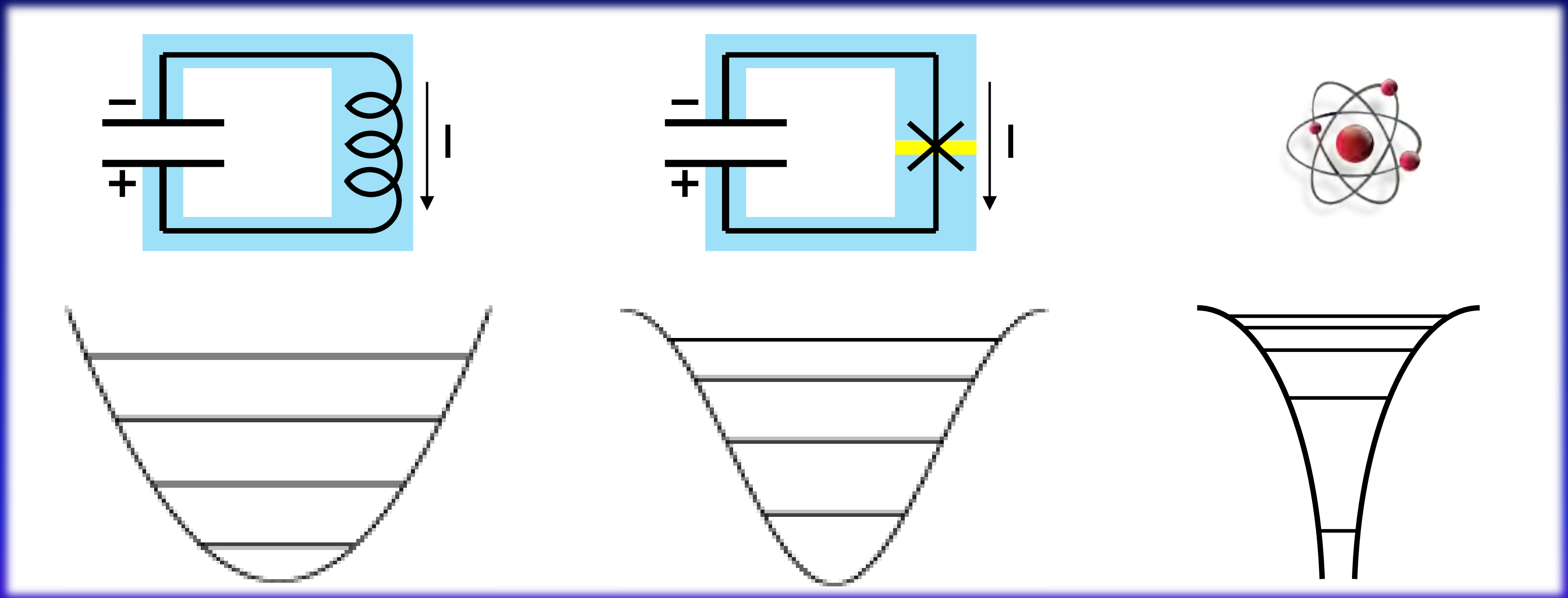

- Superconductivity ⇒ low-loss
- Josephson effect ⇒ Strong nonlinearity
- Macroscopic size ⇒ Strong coupling

Possible decoherence sources

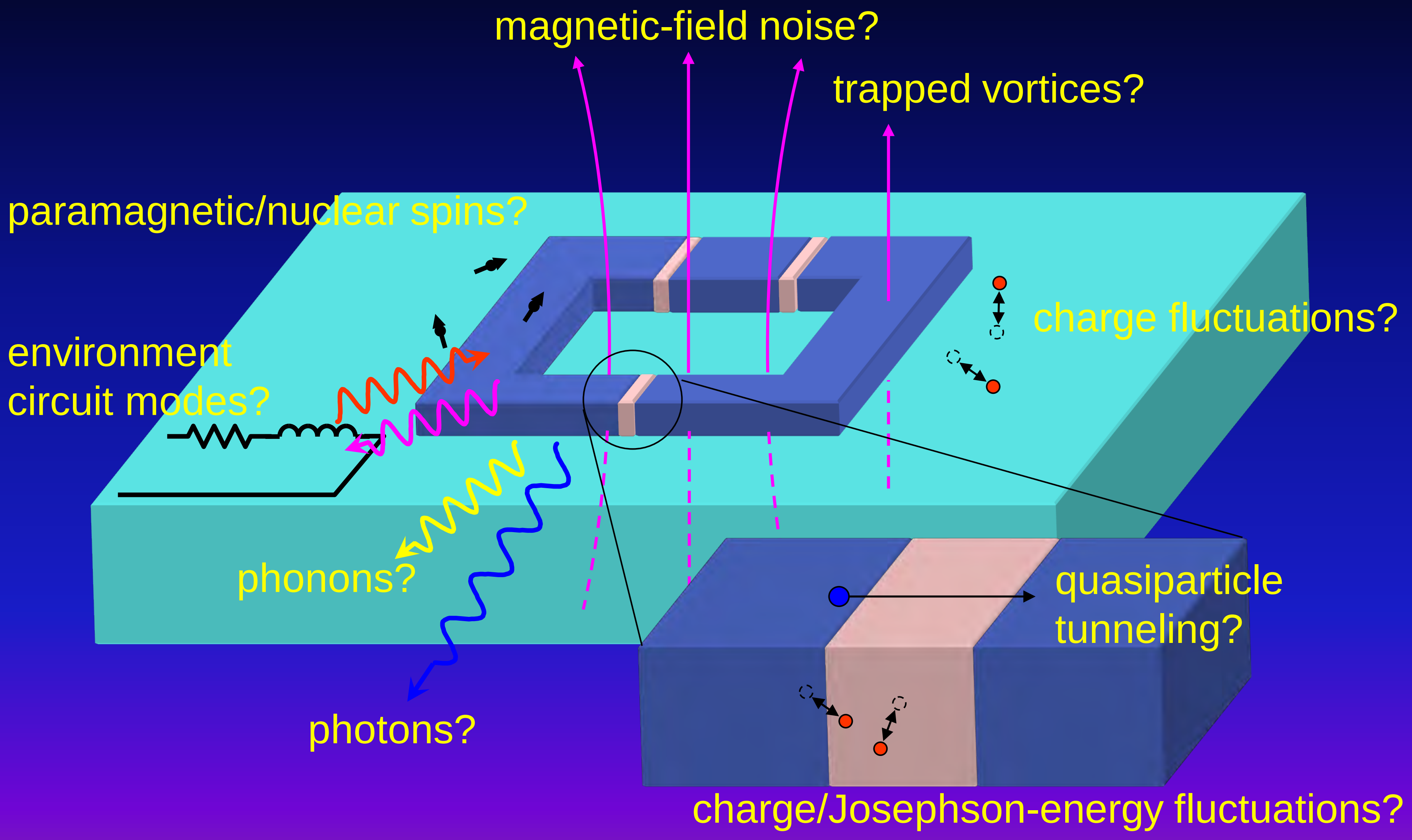

Coherence time of superconducting qubits

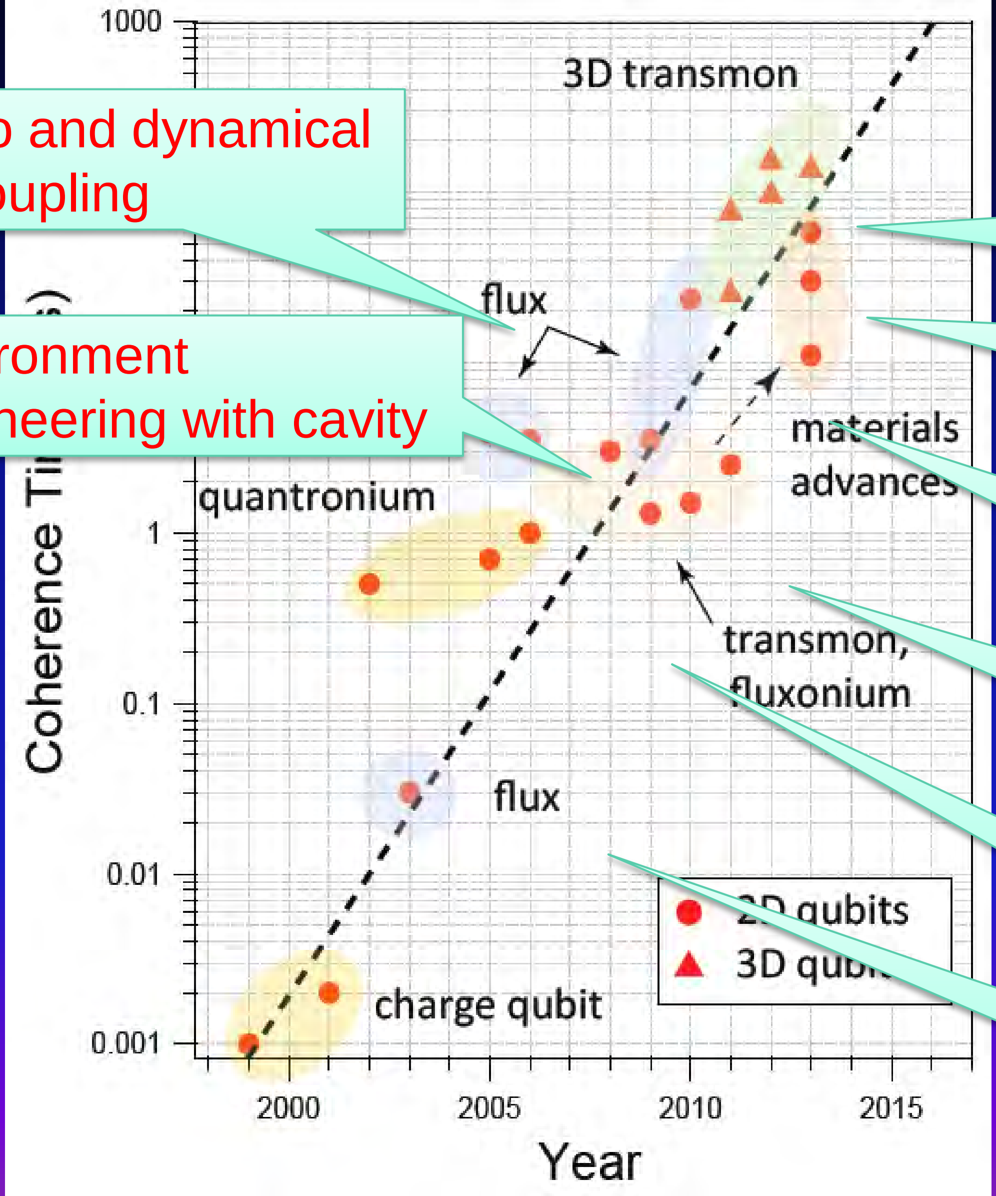

Echo and dynamical decoupling

Environment engineering with cavity

Low-energy qubit

Non-equilibrium quasiparticle engineering

High-frequency noise shielding

Diluted surface/interface effect

Improved surface/interface/dielectric

Energy-level engineering

Decoupling from charge noise

W. D. Oliver and P. Welander, MRS BULLETIN 38, 816 (2013) MIT-LL

Scaling-up superconducting quantum computers

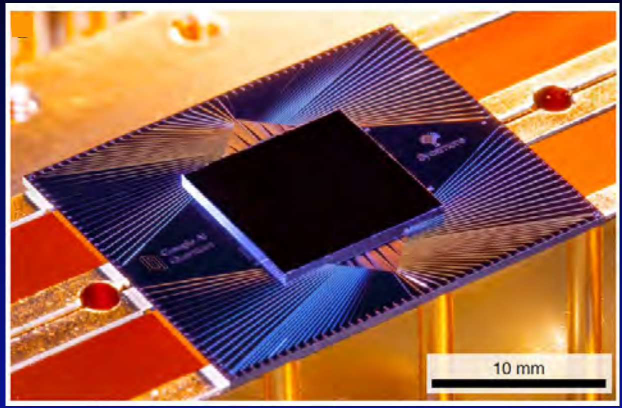

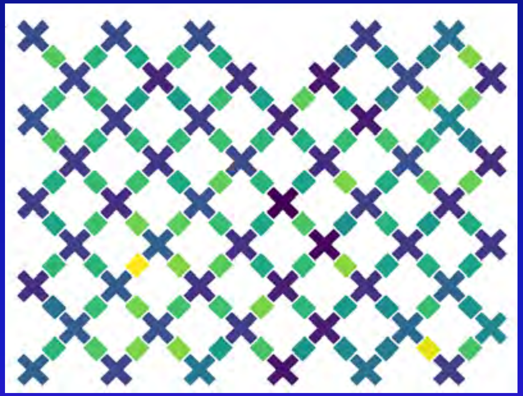

54 qubits

Google AI Quantum
Nature 574, 505 (2019)

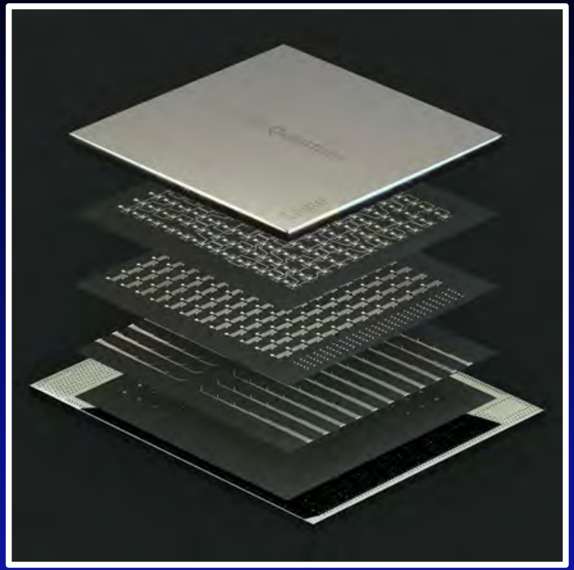

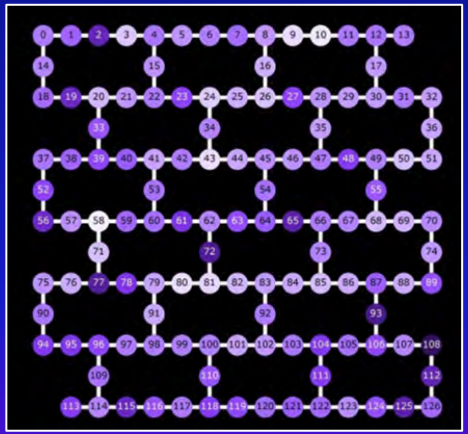

127 qubits

IBM
https://www.ibm.com/blogs/think/jp-ja/wp-content/uploads/sites/21/2021/11/IBM_ChipOpen_BLK_1000x1000.jpg

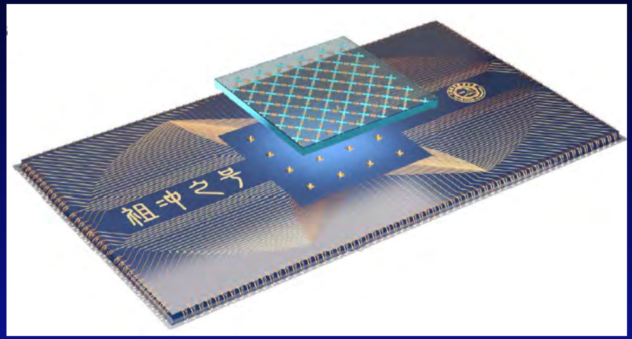

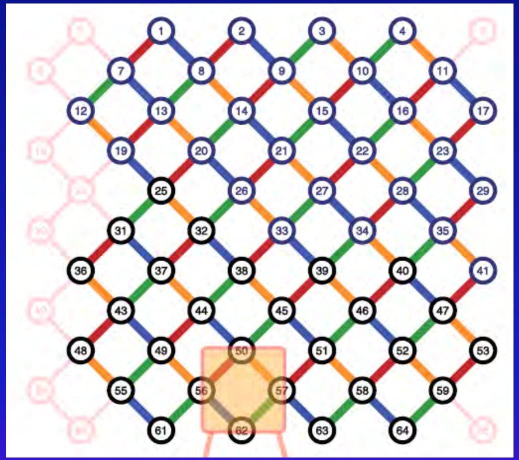

66 qubits

USTC
Phys. Rev. Lett. 127, 180501 (2021)

Scaling-up superconducting quantum computers

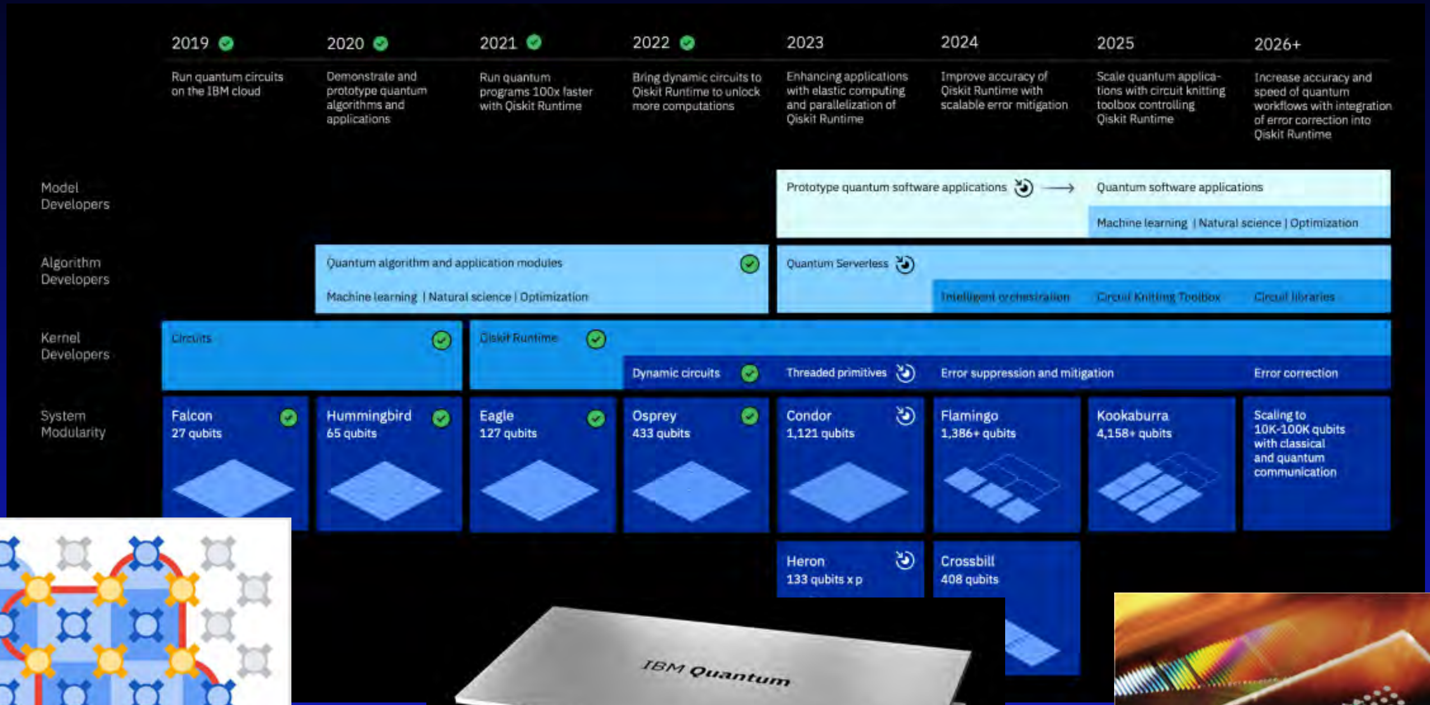

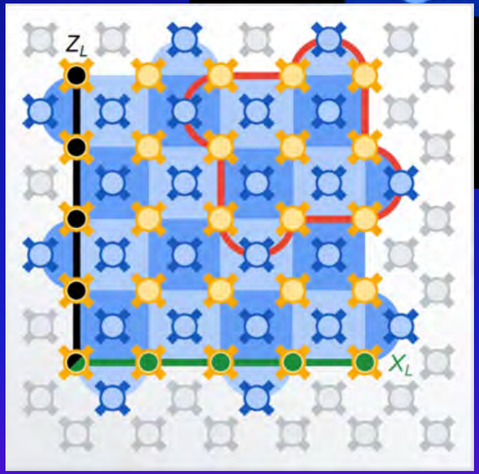

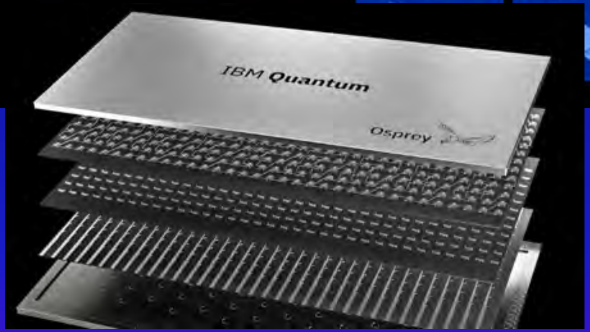

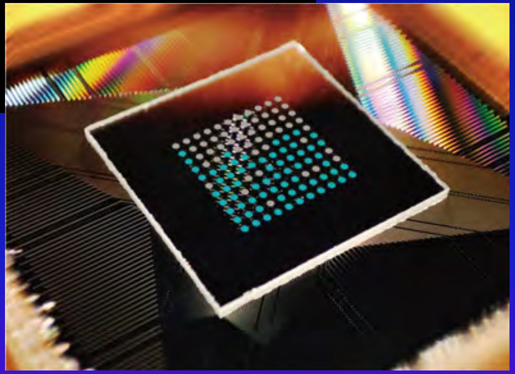

72 qubits

Google AI Quantum
arXiv:2207.06431

433 qubits

IBM
https://www.ibm.com/quantum/roadmap
https://www.youtube.com/watch?v=Szw0KwbKowI

121 qubits

Zhejiang Univ.
arXiv:2211.09802

Quantum error correcntion
and
fault-tolerant quantum computing

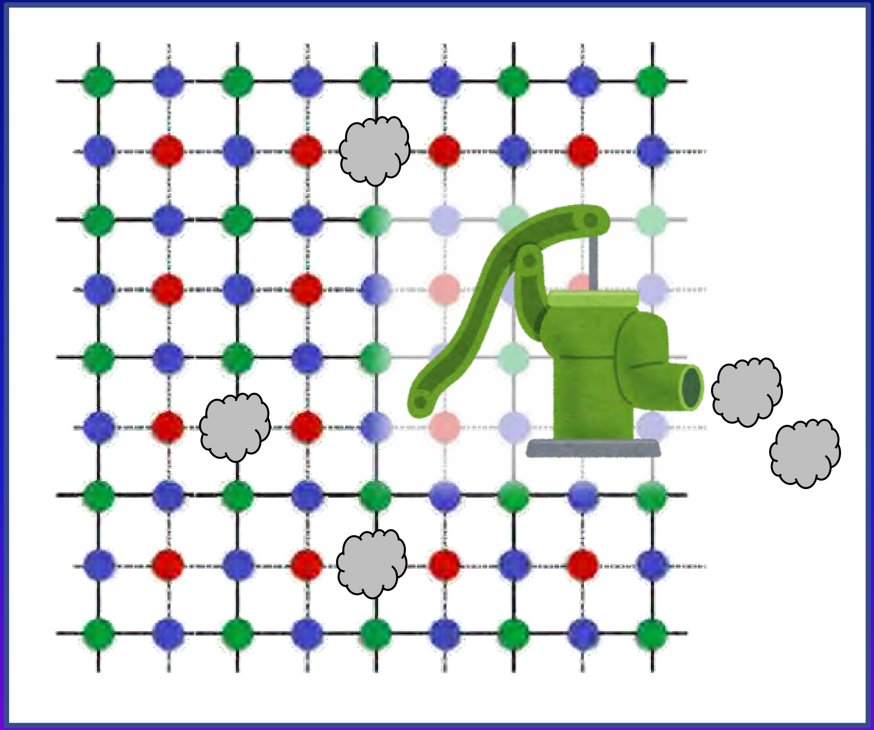

Fault-tolerant quantum computing: Surface code

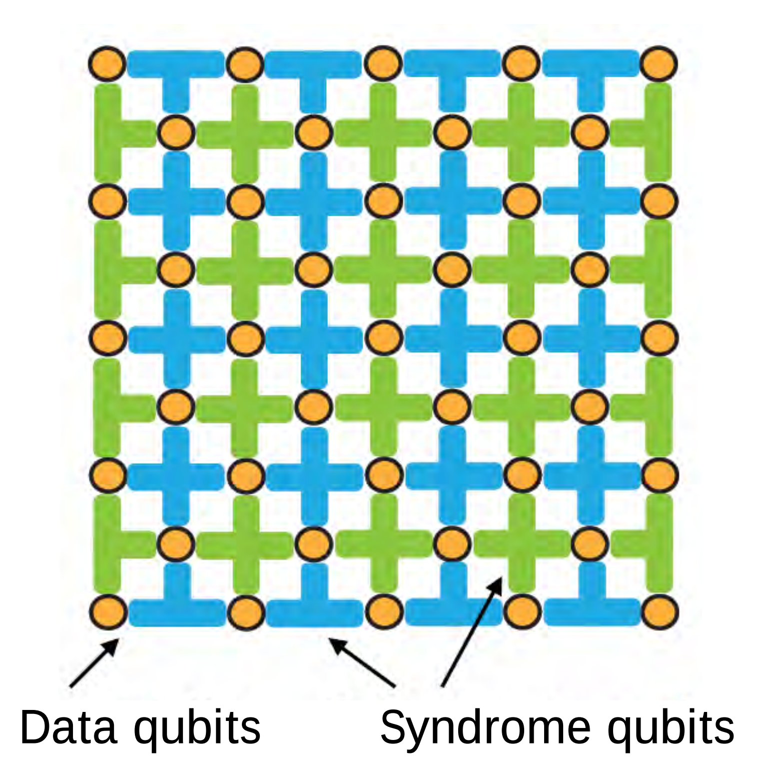

Error threshold $p_{\mathrm{th}} \sim 0.6\%$

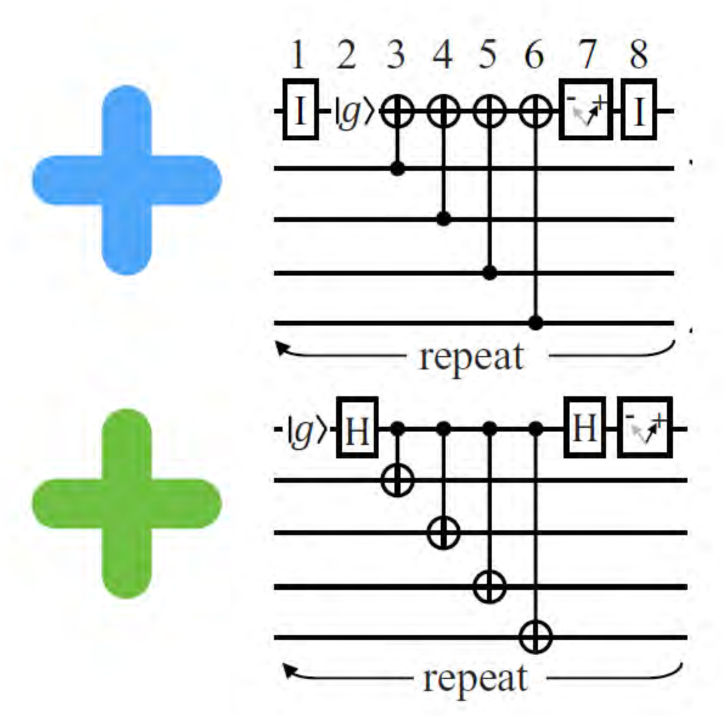

Error detection protocol

A. Fowler et al. PRA 86, 032324 (2012) UCSB

Towards quantum error correction

Not yet break-even

Surface code d=3

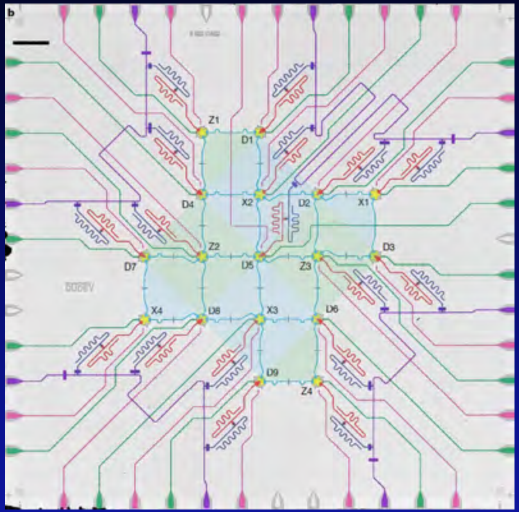

ETH Zurich
Nature 605, 669 (2022)

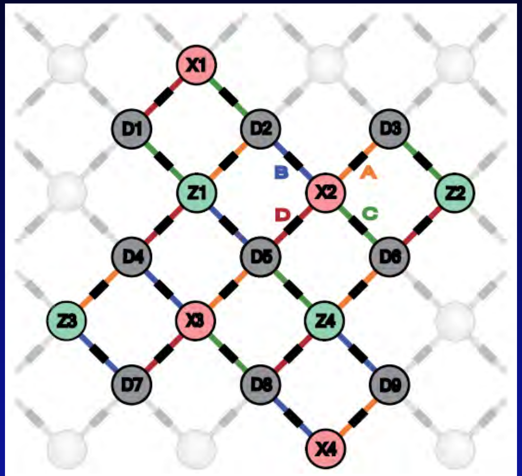

USTC
Phys. Rev. Lett. 129, 030501 (2022)

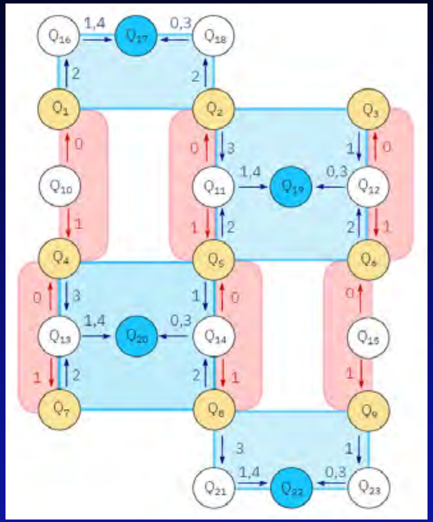

IBM
arXiv:2203.07205

Surface code d=5

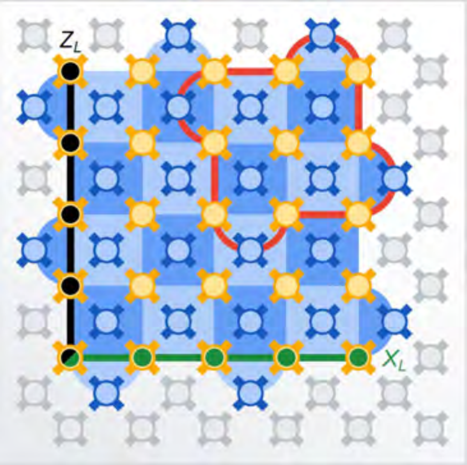

Google AI Quantum
arXiv:2207.06431

Braiding operation

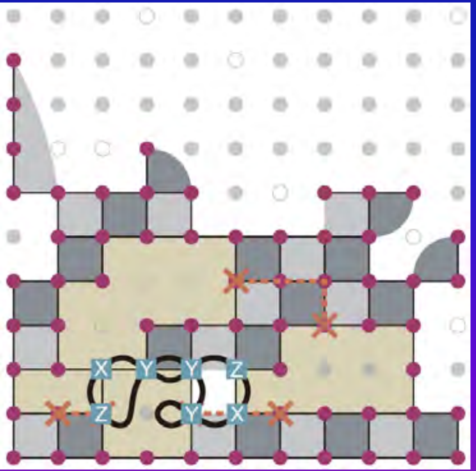

Zhejiang Univ.
arXiv:2211.09802

2D integration with 3D wiring

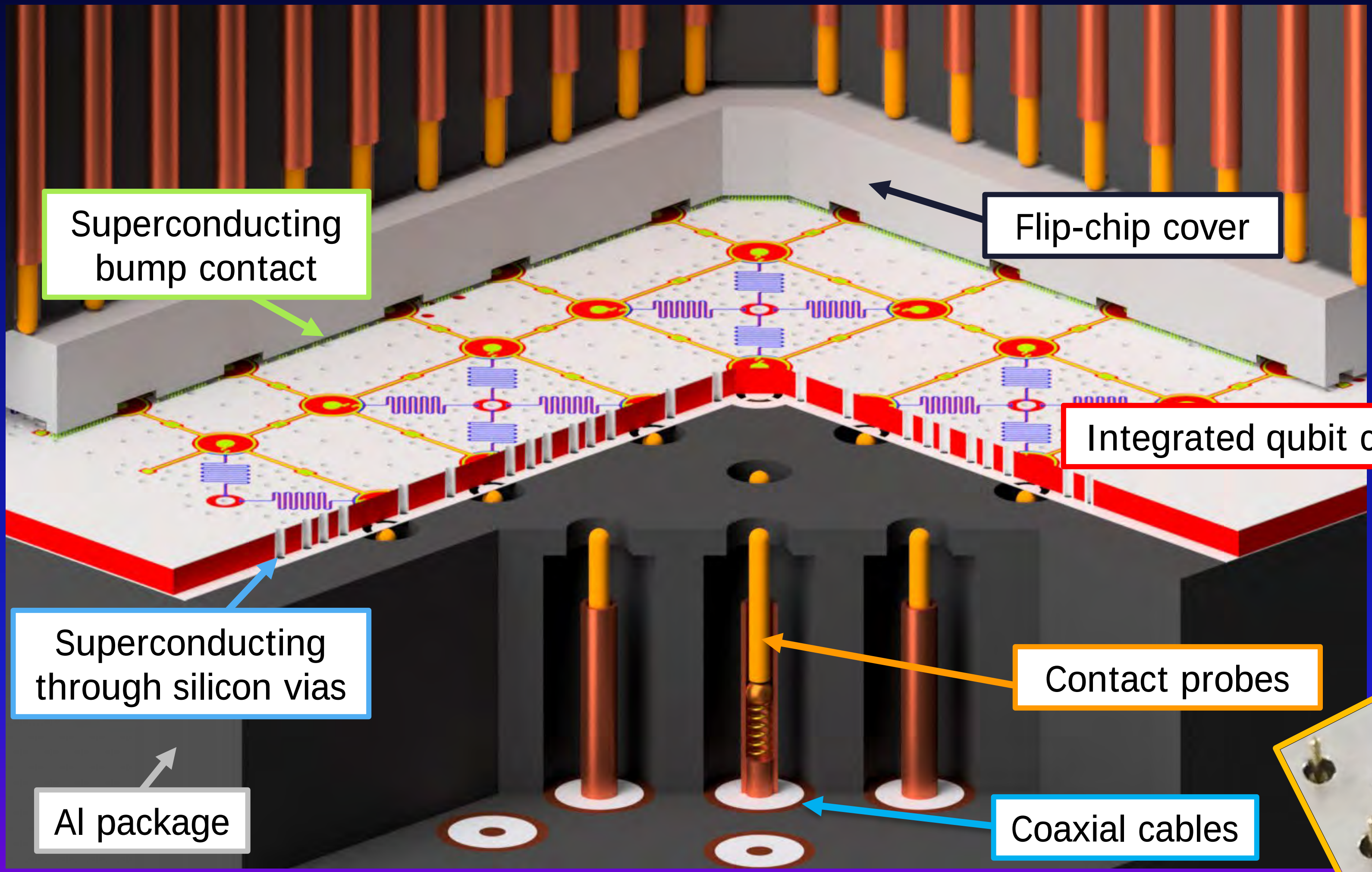

16-qubit chip

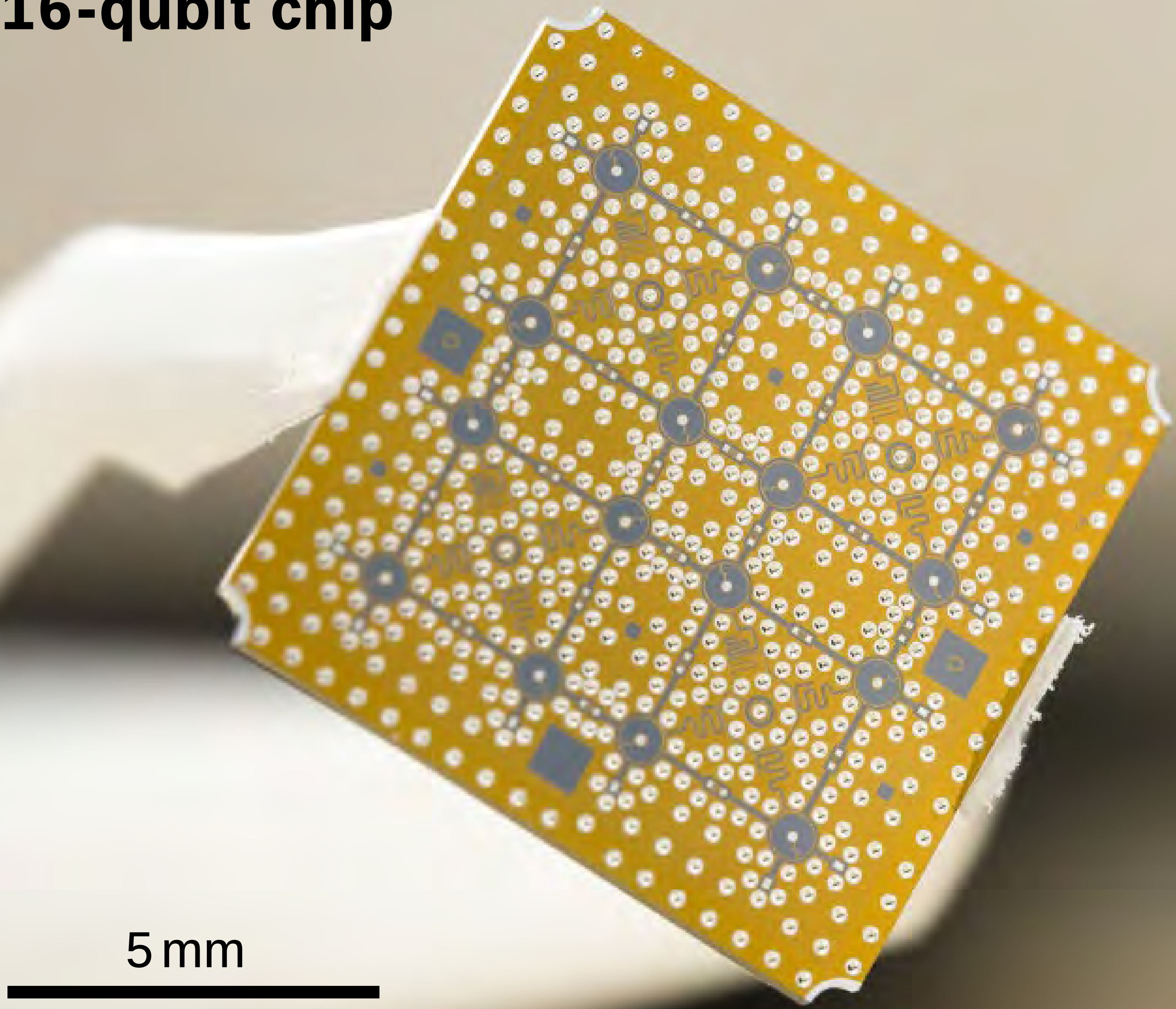

64-qubit chip

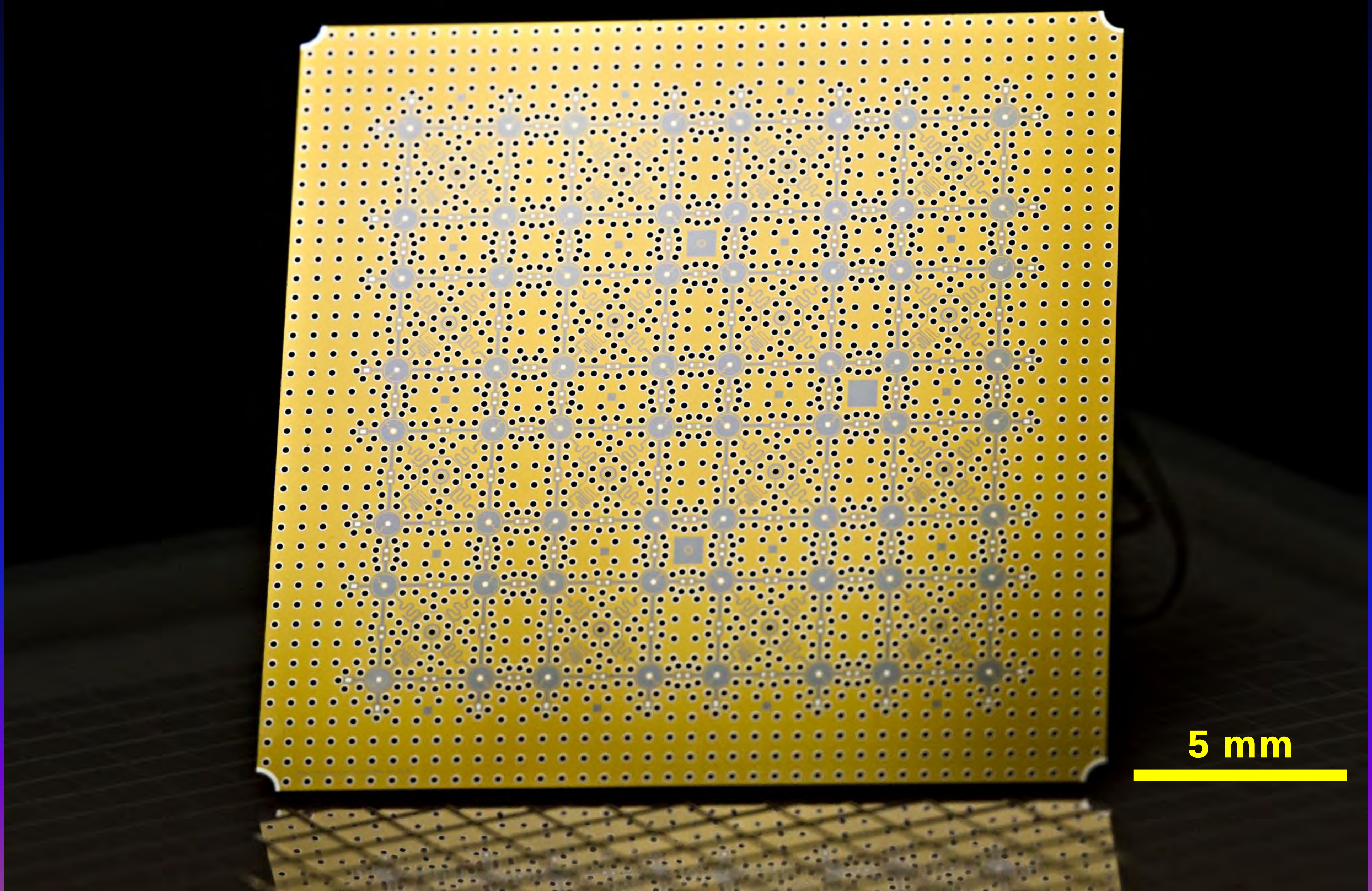

Unit cell structure

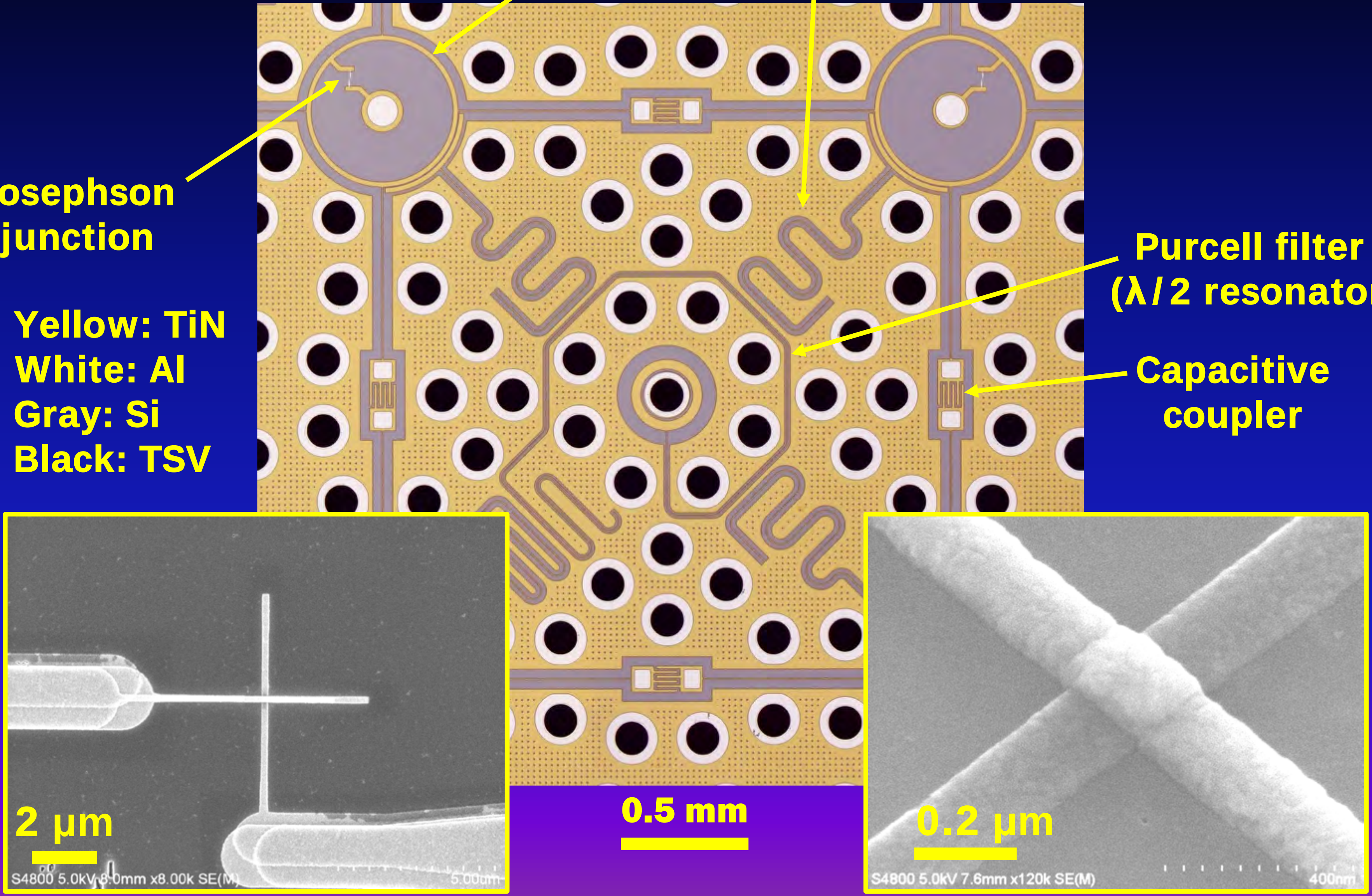

Unit cell structure ユニットセル構造

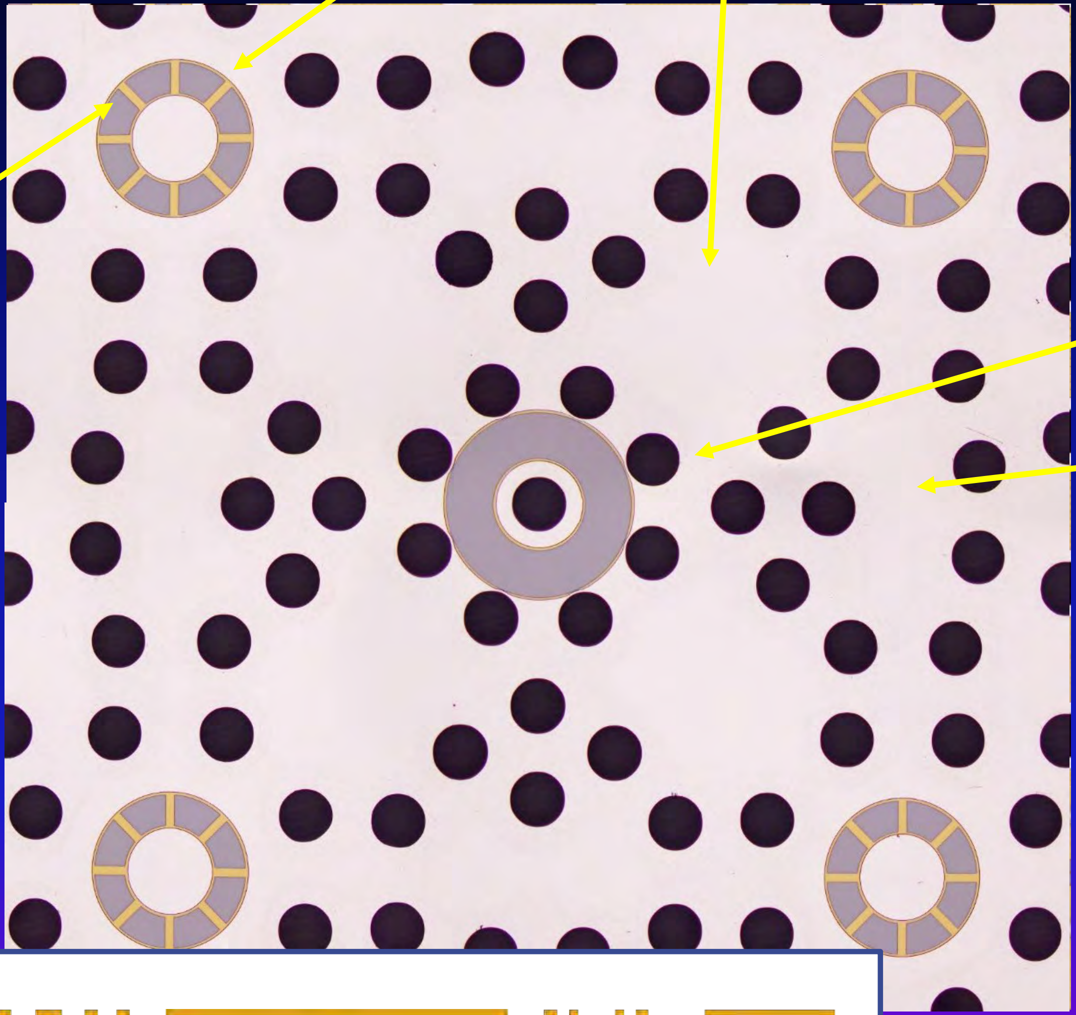

Yellow: TiN
White: Al
Gray: Si
Black: TSV

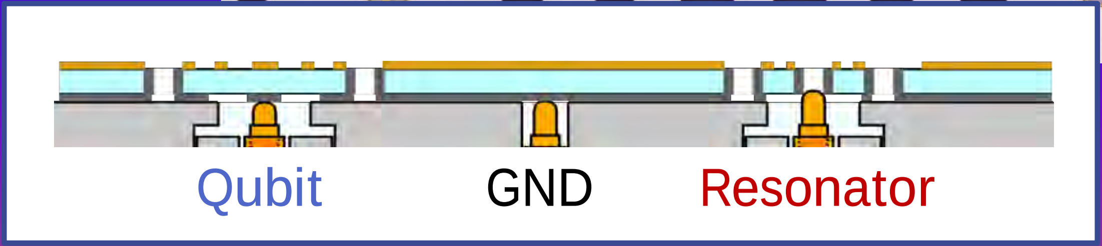

Single-qubit gate

$$\frac{H}{\hbar} = \frac{\omega_{\mathrm{q}}}{2}\sigma_z + \Omega_{\mathrm{R}} \cos\omega_{\mathrm{q}} t\, \sigma_x$$

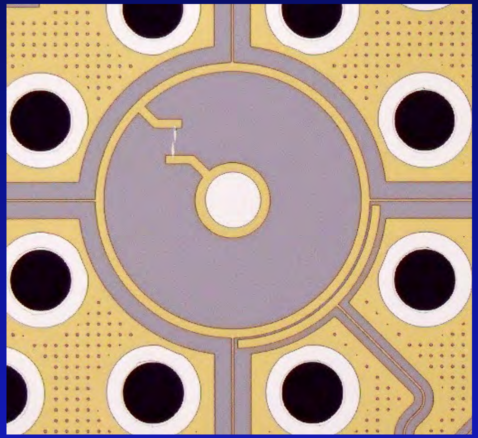

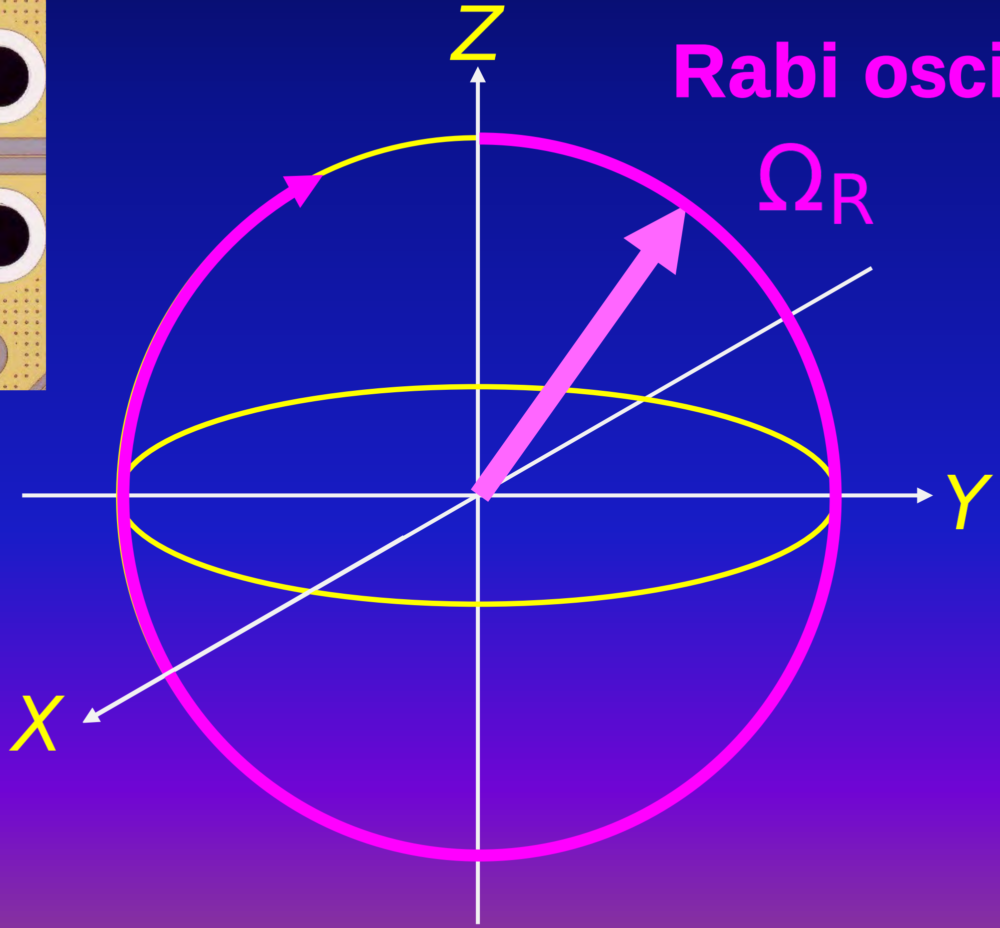

Rabi oscillation

X gate

Two-qubit gate

$$\frac{H}{\hbar} = \frac{\omega_{q1}}{2}\sigma_{z1} + \frac{\omega_{q2}}{2}\sigma_{z2} + g\sigma_{x1}\sigma_{x2}$$

$$+\Omega_{CR}\cos\omega_{q2}t\,\sigma_{x1} \qquad \Delta_{12} \equiv \omega_{q1} - \omega_{q2} \gg g$$

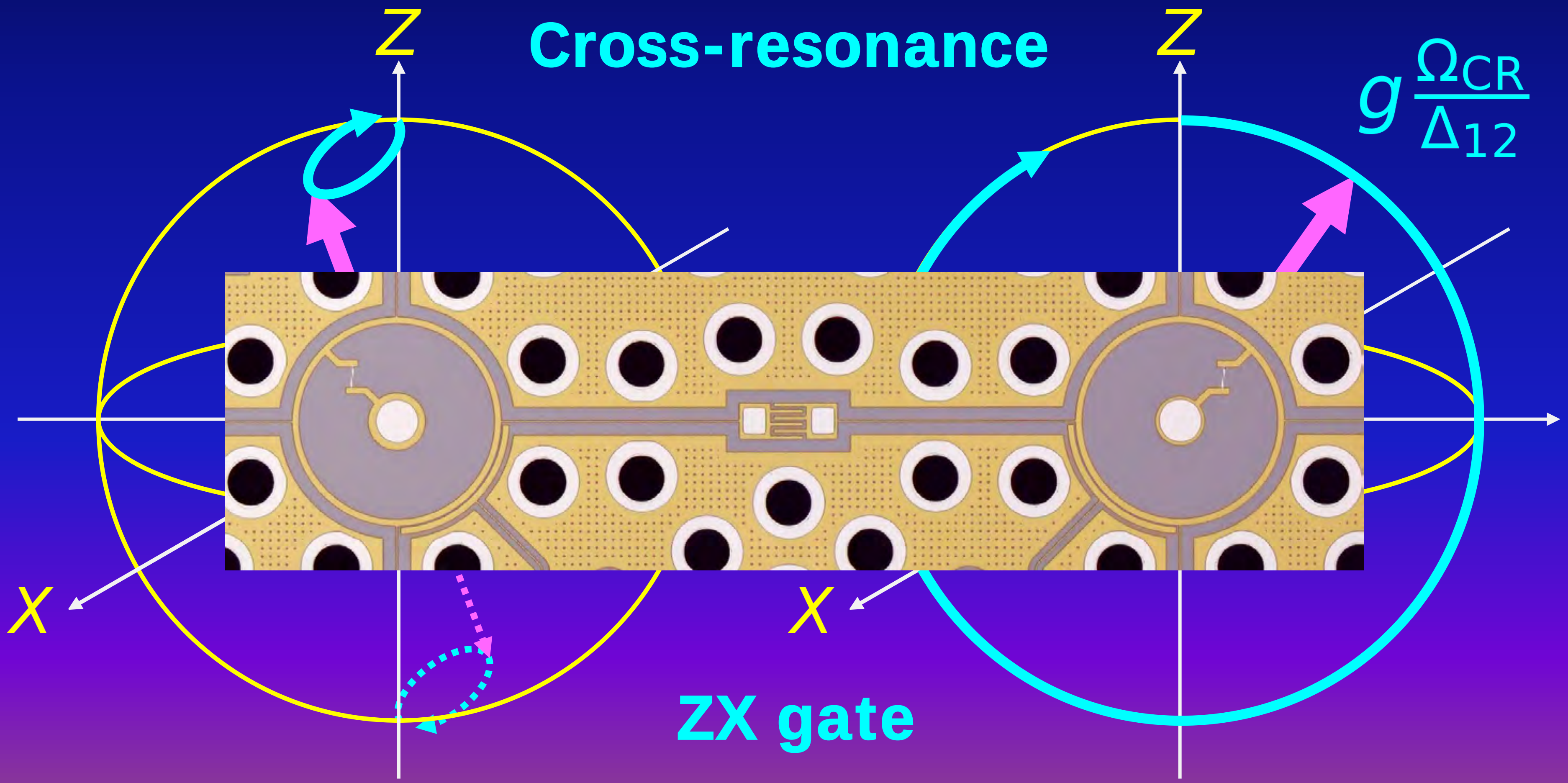

Qubit readout

$$H_{\mathrm{JC}} = \frac{\hbar\omega_{\mathrm{q}}}{2}\hat{\sigma}_z + \hbar\omega_{\mathrm{c}}\hat{a}^\dagger\hat{a} + \hbar g(\hat{\sigma}_+\hat{a} + \hat{\sigma}_-\hat{a}^\dagger)$$

Cavity mode   Interaction

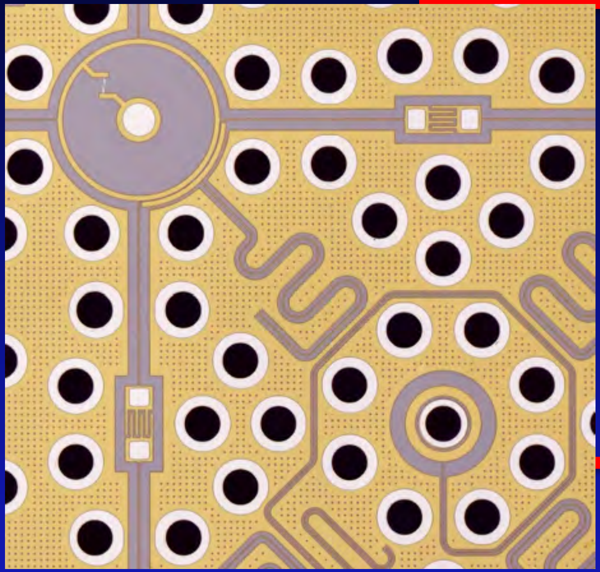

$(\Delta \equiv \omega_{\mathrm{q}} - \omega_{\mathrm{c}},\ \ \chi = g^2/\Delta)$

$$\frac{\hbar(\omega_{\mathrm{q}} - \chi)}{2}\hat{\sigma}_z + \hbar\omega_{\mathrm{c}}\hat{a}^\dagger\hat{a} - \hbar\chi\hat{a}^\dagger\hat{a}\hat{\sigma}_z$$

Qubit   Cavity mode   Interaction

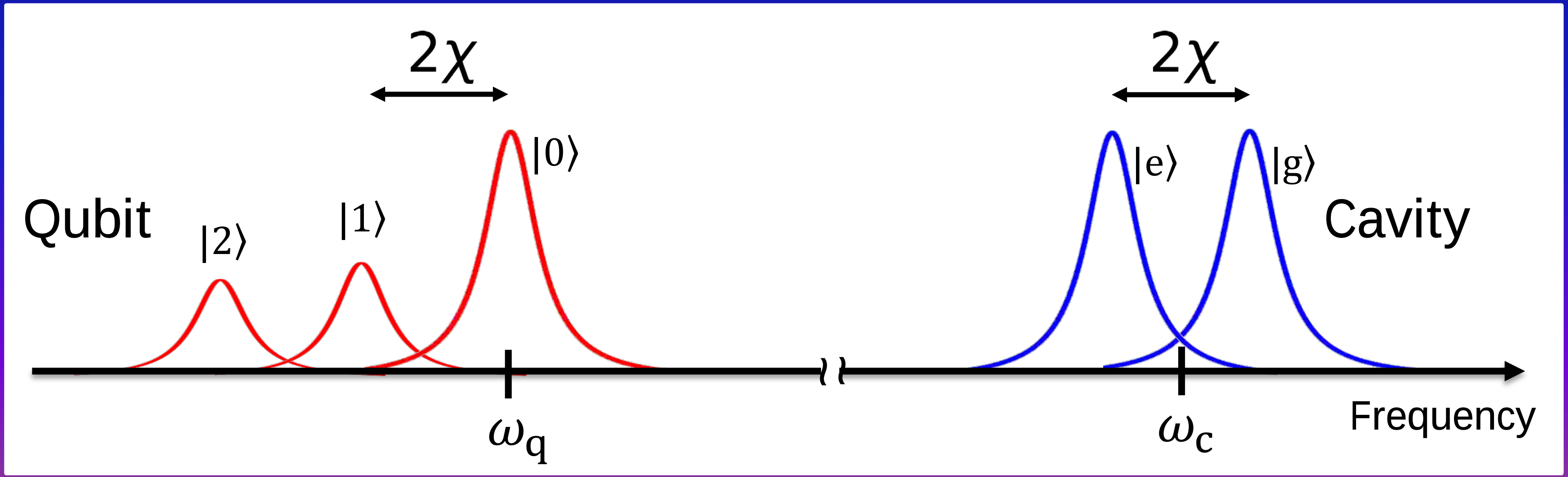

Packaging with vertical access

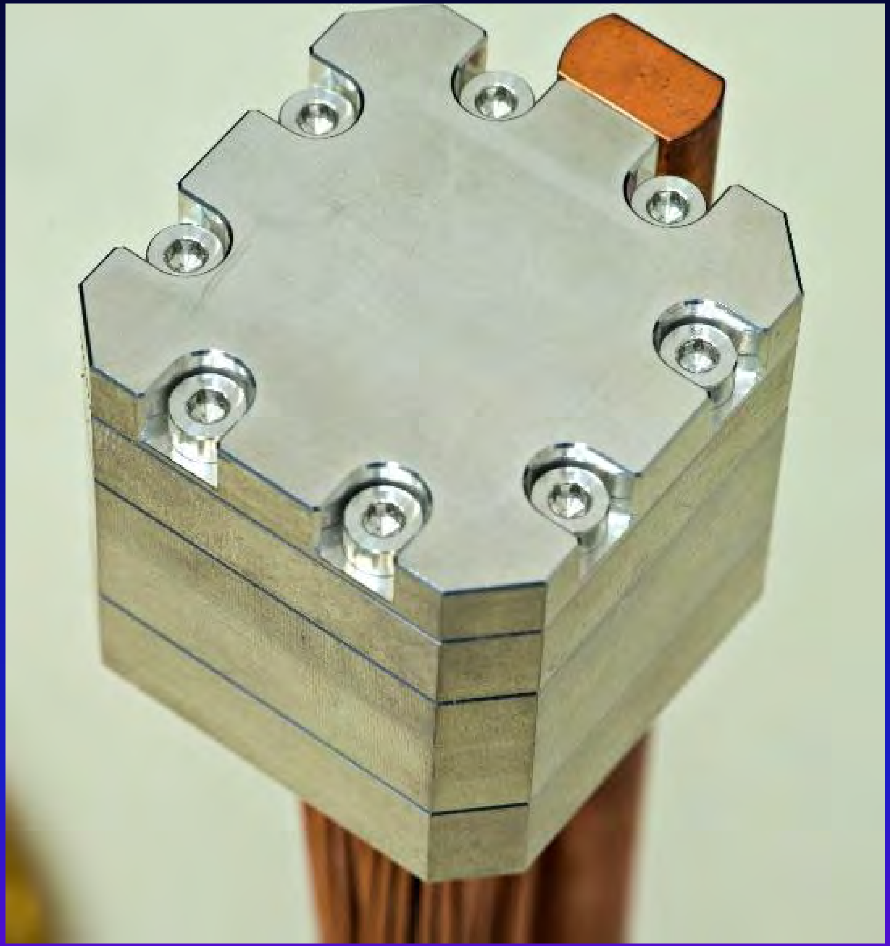

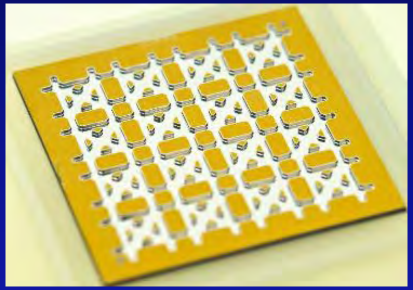

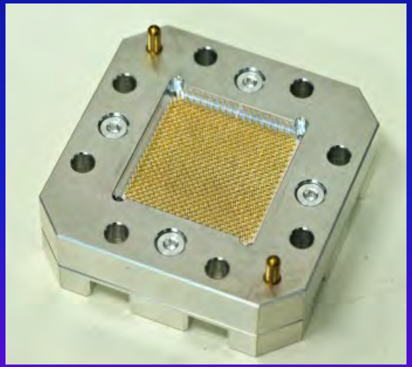

Cryostat for 64Q system

- Input 96 lines*
  Output 16 lines
  Total 112 lines
- 16 low-temperature HEMT amplifier
- 16 Impedance-matched Josephson parametric amplifier (JPA)
- Magnetic shield
- Radiation shield at 10 mK

* Qubit control	64
Readout signal input	16
JPA pump	16

Custom-made control system for 64Q system

大阪大学
OSAKA UNIVERSITY

Control and readout fidelities

Coherence time	: T_1 ~ 40 µs, T_{2E} ~ 60 µs
Single-shot readout	: 0.990 (~350 ns)
Initialization	: 0.997
Single-qubit gate	: 0.9996 (~17 ns)
Two-qubit gate	: 0.991 (~170 ns)

Best values

Single-shot readout

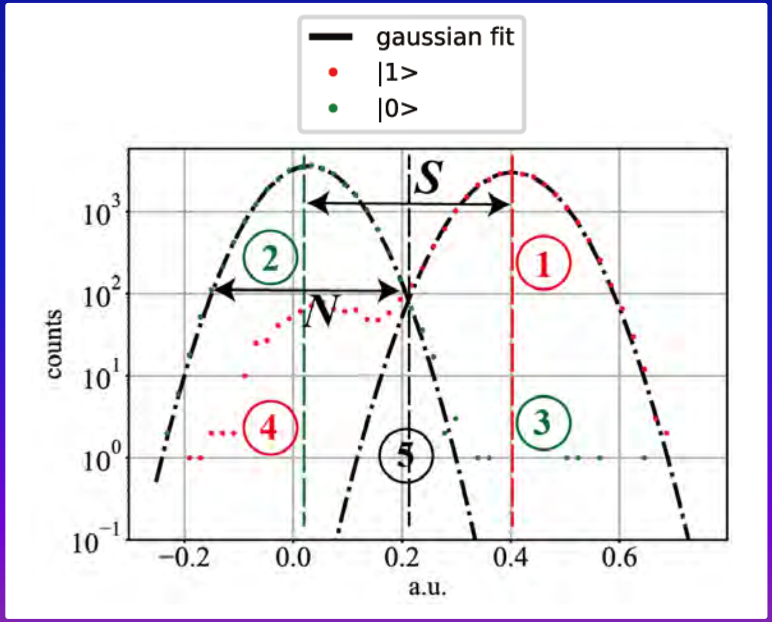

Single-qubit gate

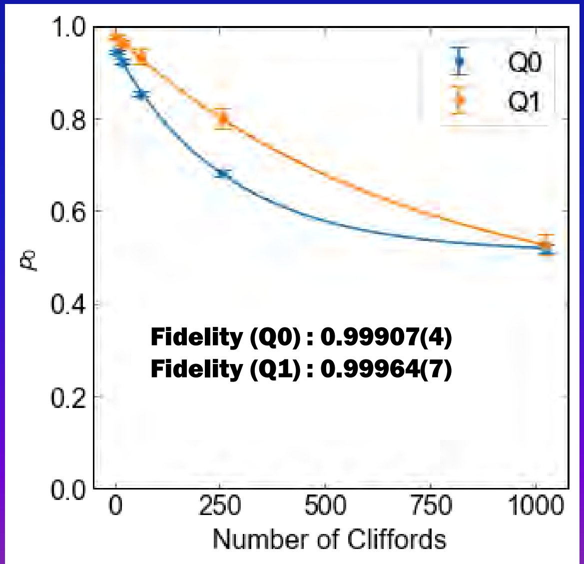

Two-qubit gate (cross resonance)

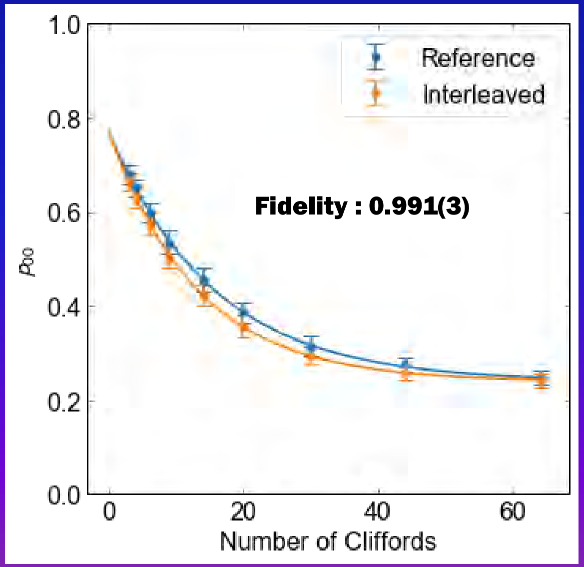

Tentatively operable qubits

Estimation from measured qubit parameters

Broken qubit

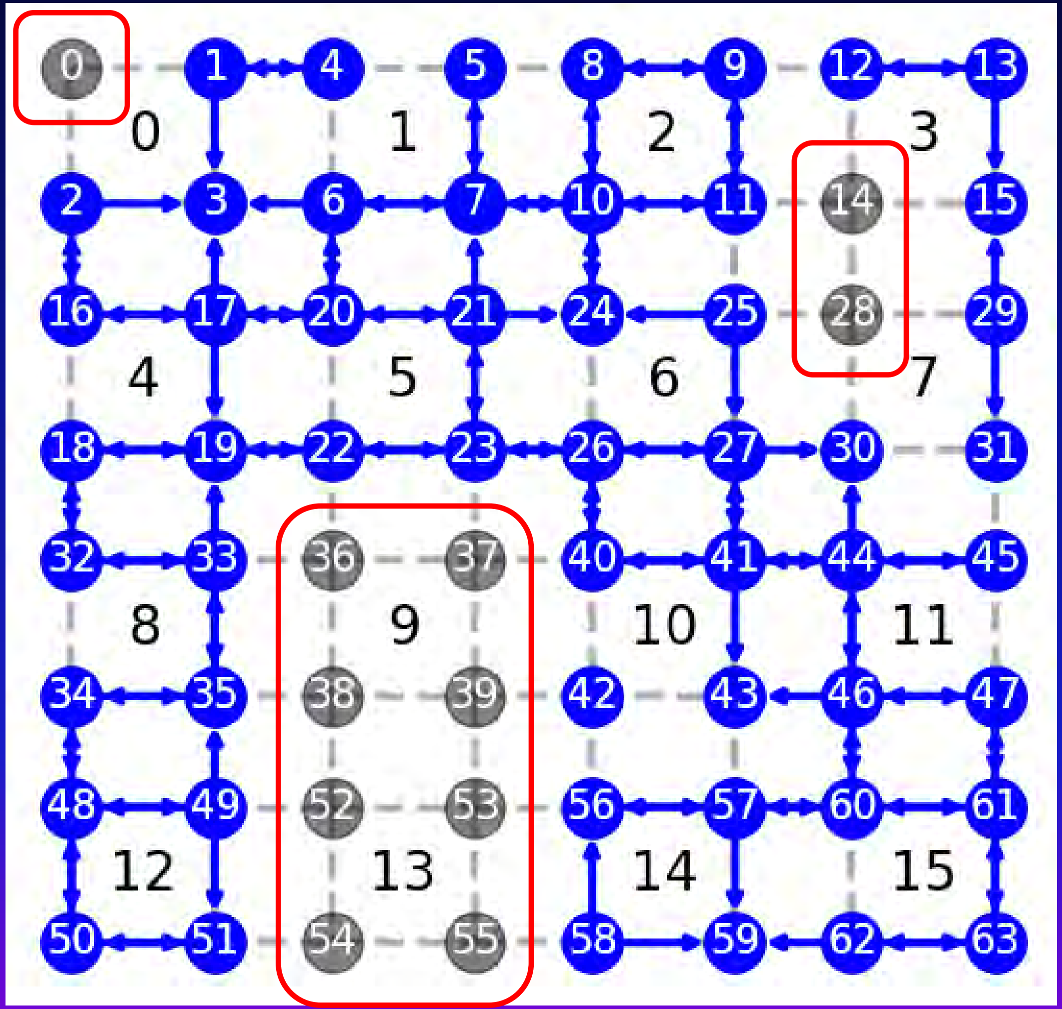

Frequency-collision qubit pair

Coherence times:
T_1 ~ 10-20 μs
T_{2E} ~20-40 μs

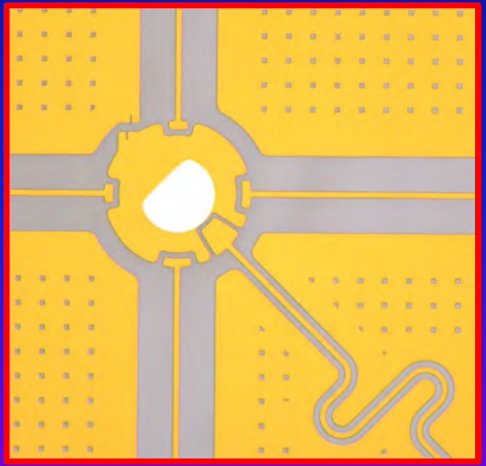

Grounded transmon
with floated coupling buses

HEMT wiring issues (?)

Microwave quantum optics: Cavity QED and waveguide QED

Cavity QED

Atom + 0D mode (discrete)

Strong coupling

$$g \gg \kappa, \gamma, \gamma_\varphi$$

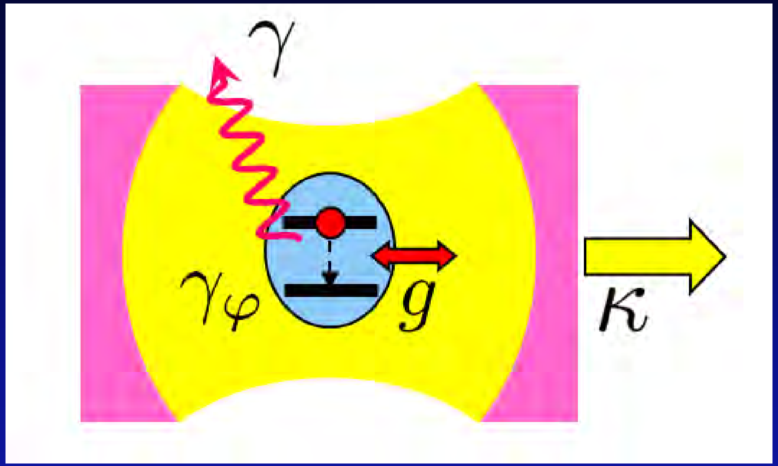

Waveguide QED

Atom + 1D mode (continuum)

Mode matching, interference

"Strong coupling"

$$\Gamma_1 \gg \gamma, \gamma_\varphi$$

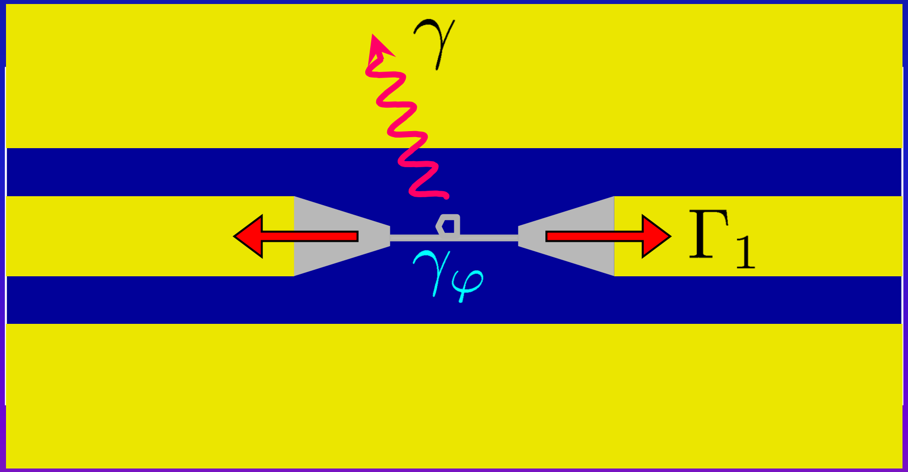

O. Astafiev et al. Science 327, 840 (2010)

Quantum nondemolition detection of microwave photons

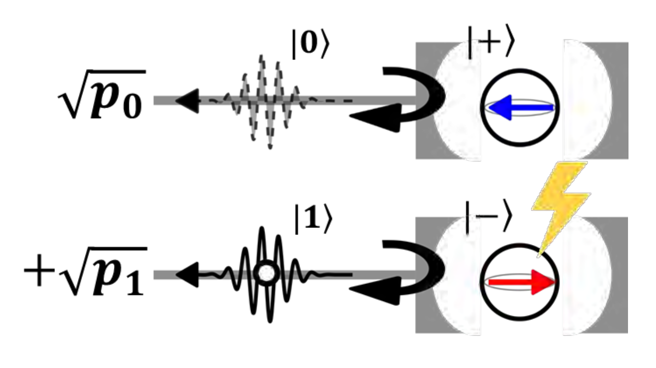

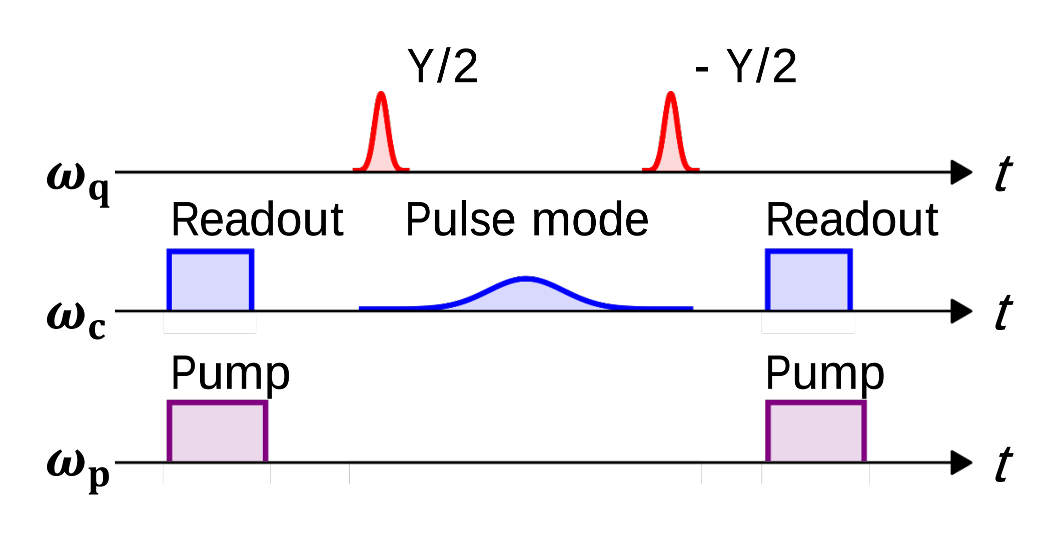

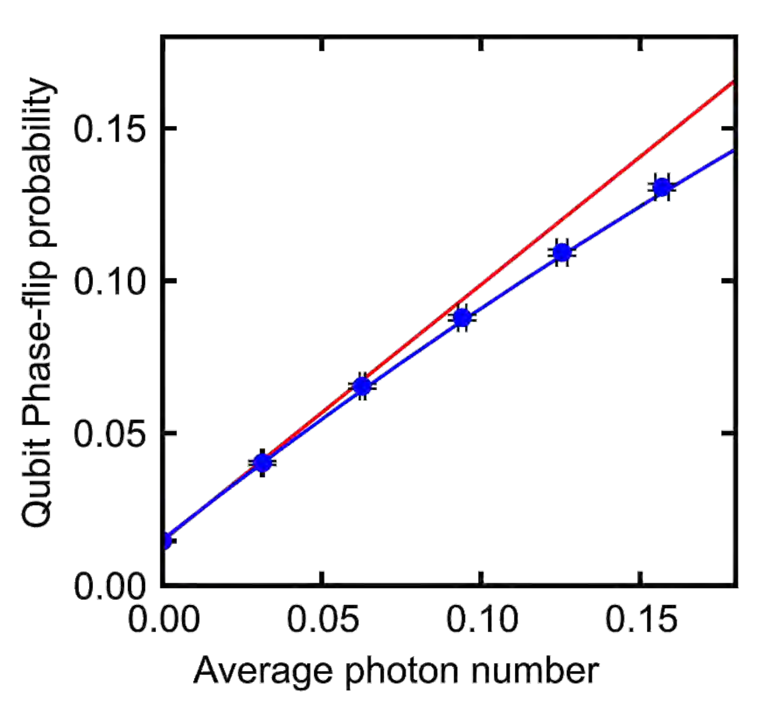

S. Kono et al. Nature Phys. 14, 546 (2018)

- **Dark count probability**
  P_{dc} = 0.0147
- **Quantum efficiency**
  η = 0.84

  - **Internal loss of the cavity**
  - **Dephasing**
  - **Mismatch of κ and 2χ**

Conditional Wigner tomography

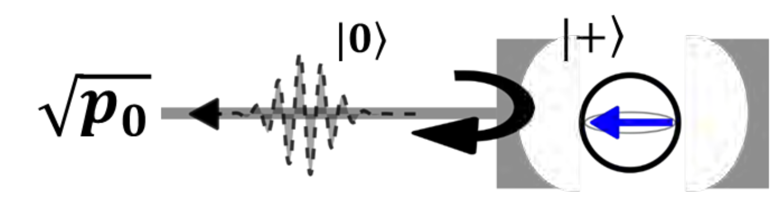

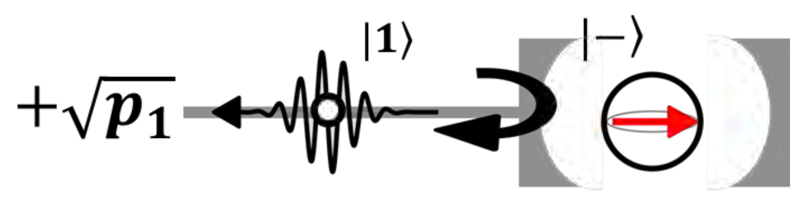

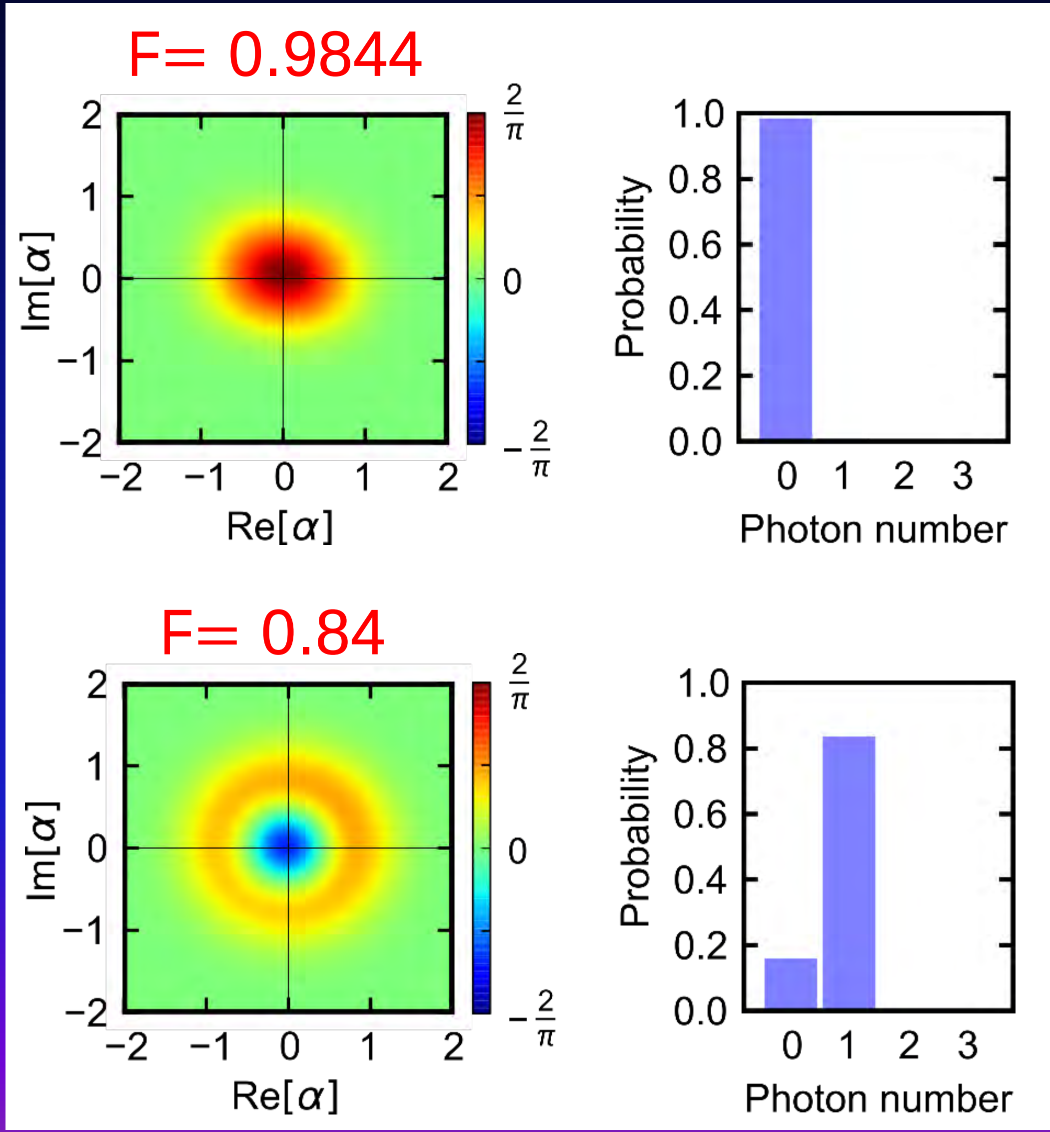

Corrected for $\eta_{det} = 0.43$

S. Kono et al. Nature Phys. 14, 546 (2018)

Qubit readout with intrinsic Purcell filter

2D implementation

- **Readout time 36 ns**
- **Readout fidelity 99.62%**
- **QND fidelity 99.63%**

$\omega_q/2\pi$=8.09 GHz
$\omega_r/2\pi$=9.25 GHz

T_1= 40 μs

$\kappa/2\pi$=66 MHz
$\chi/2\pi$=-5.5 MHz

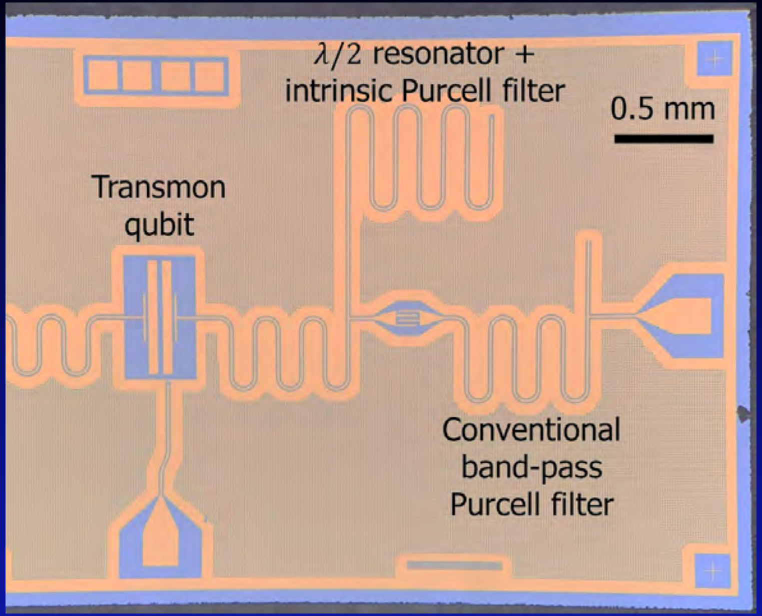

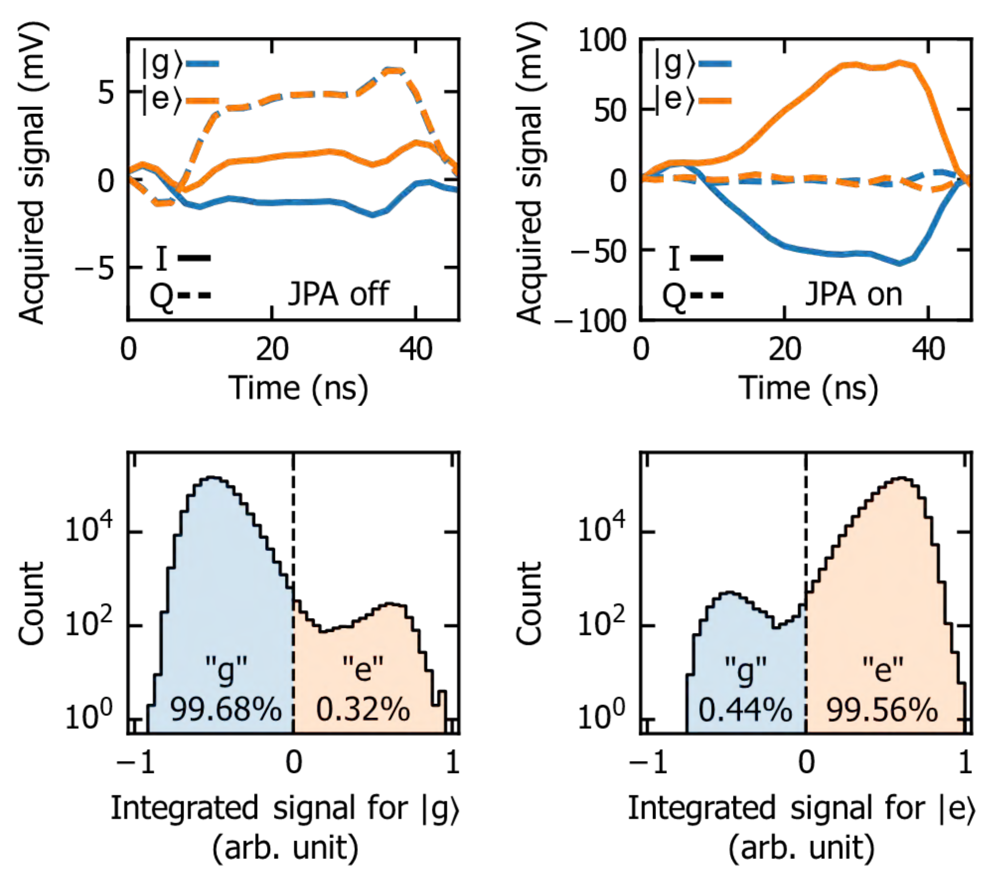

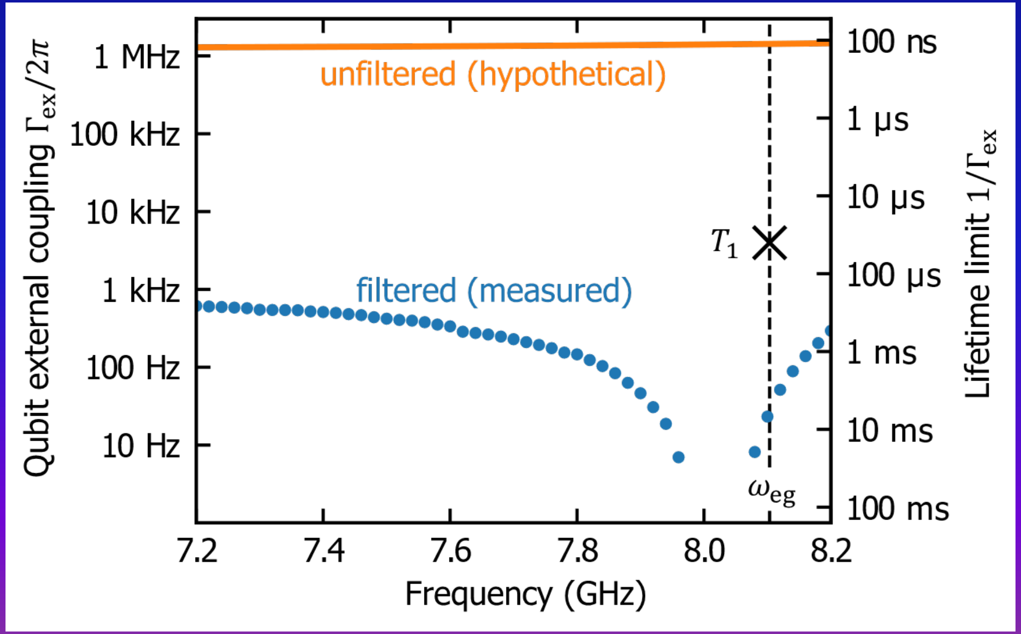

Y. Sunada

Hybrid quantum systems using collective modes

Superconducting quantum electronics

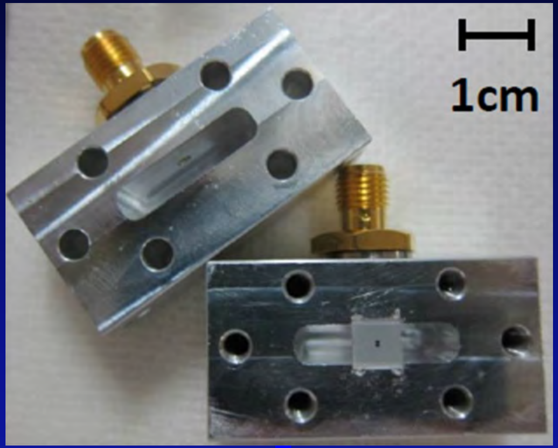

Nonlinearity

Quantum magnonics

Quantum nanomechanics+acoustics

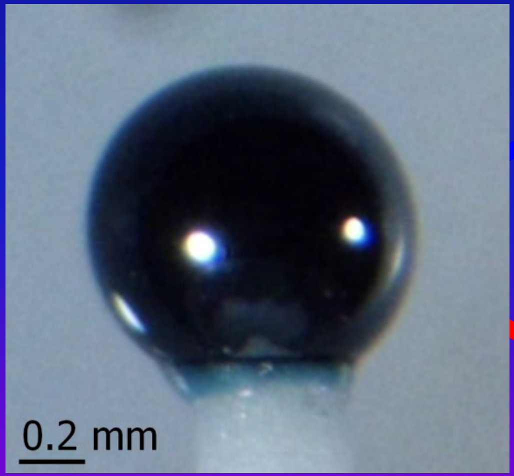

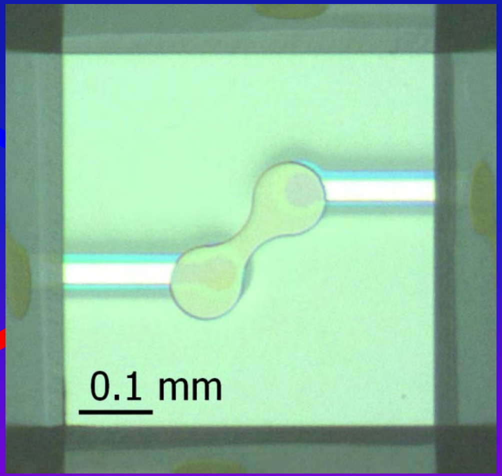

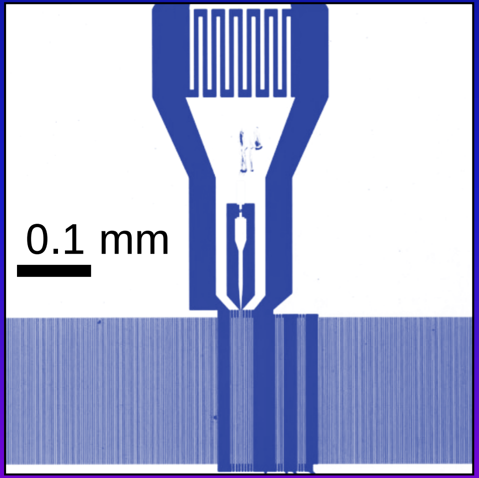

Quantum magnonics

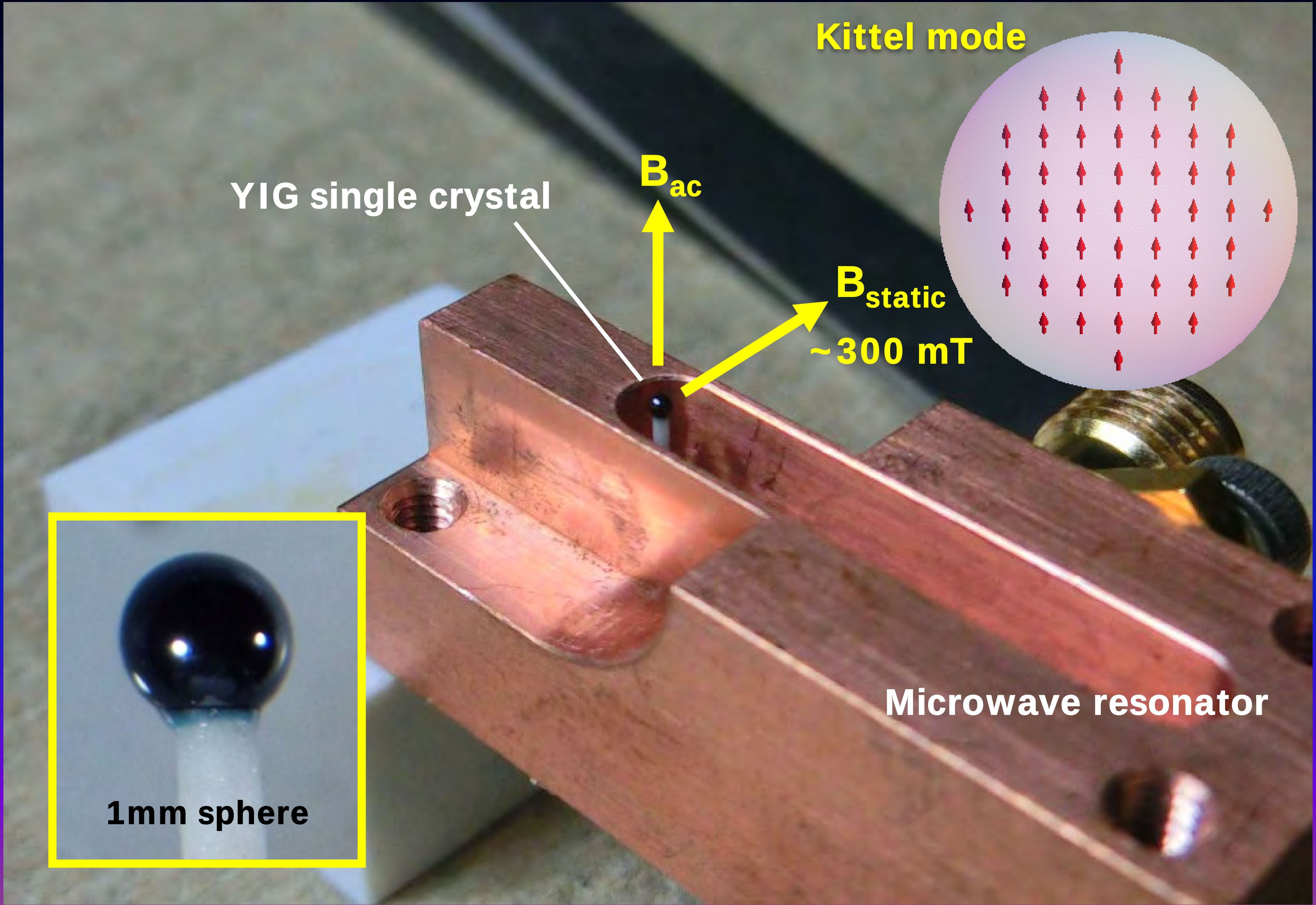

Coupling with a superconducting qubit

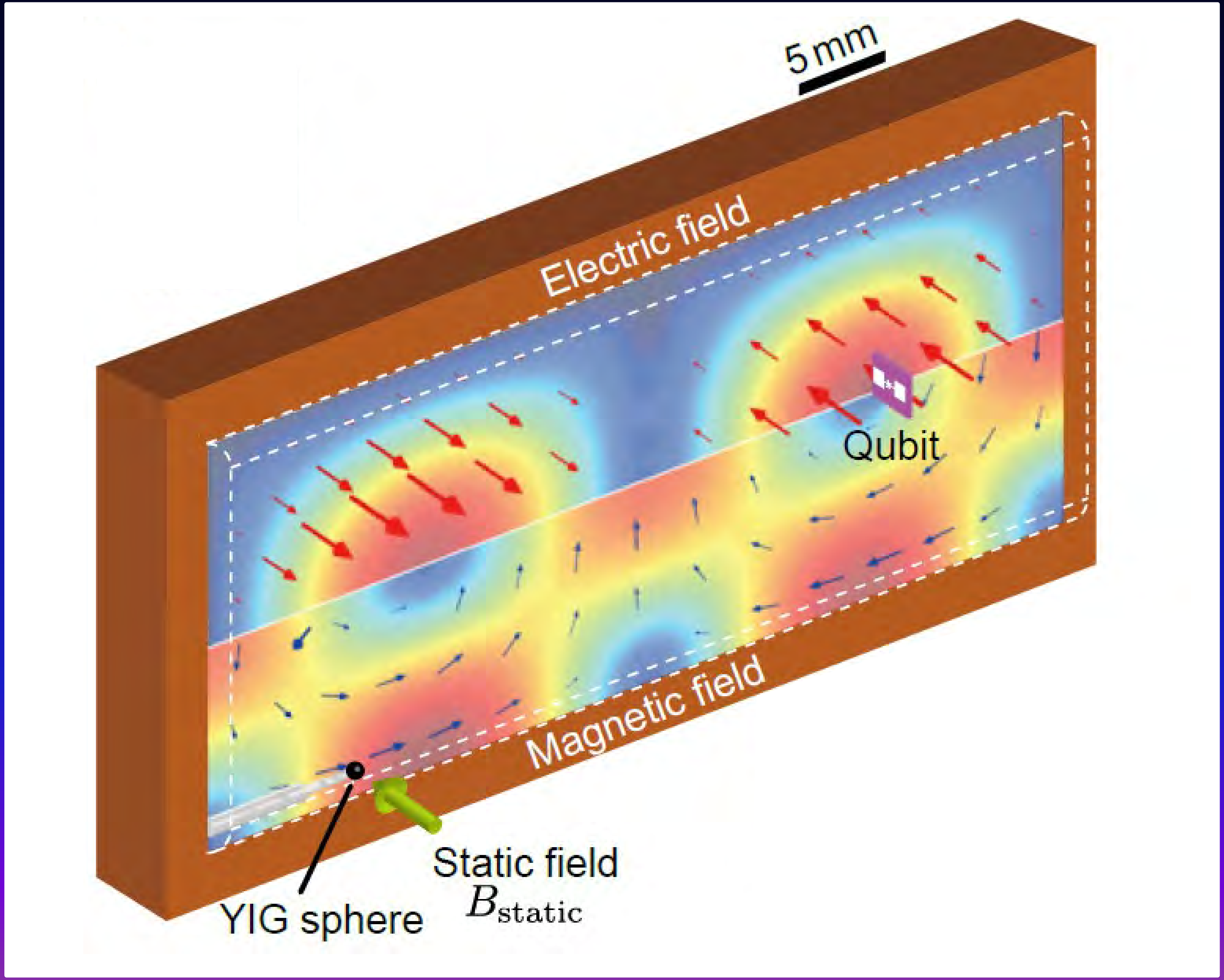

Vacuum Rabi splitting

$$\hat{\mathcal{H}}_{\text{q-m}}/\hbar \sim g_{\text{q-m}}\left(\hat{a}^{\dagger}_{\text{m}}\hat{\sigma}_{-} + \hat{a}_{\text{m}}\hat{\sigma}_{+}\right)$$

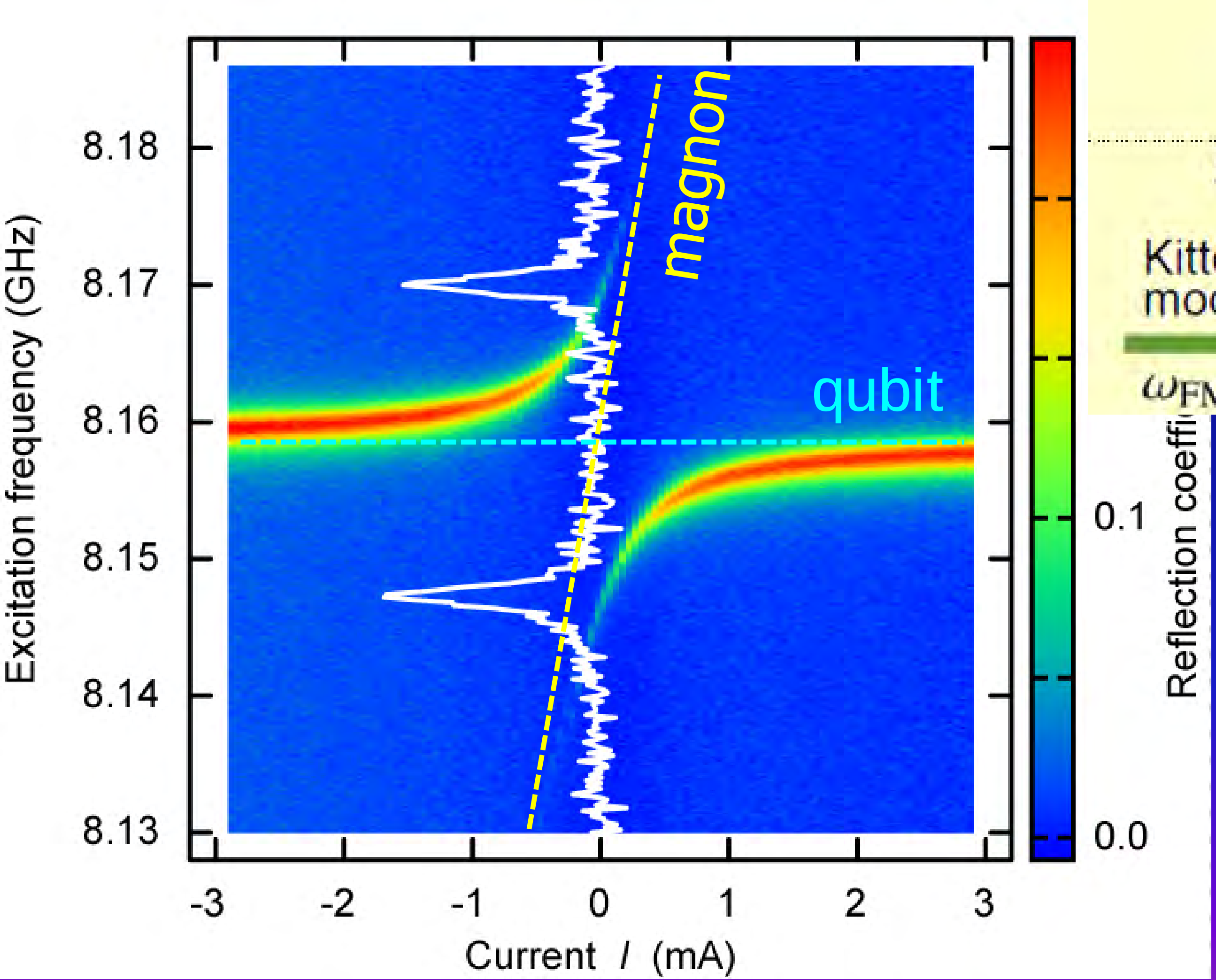

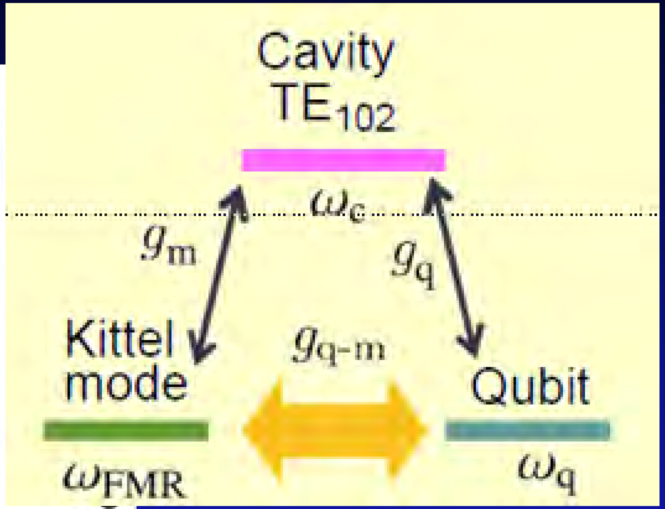

Y. Tabuchi et al. Science 349, 405 (2015)

Magnon-number-resolving spectroscopy

Strong dispersive regime $2|\chi_{\text{q-m}}| \gg \gamma_{\text{q}}, \gamma_{\text{m}}$

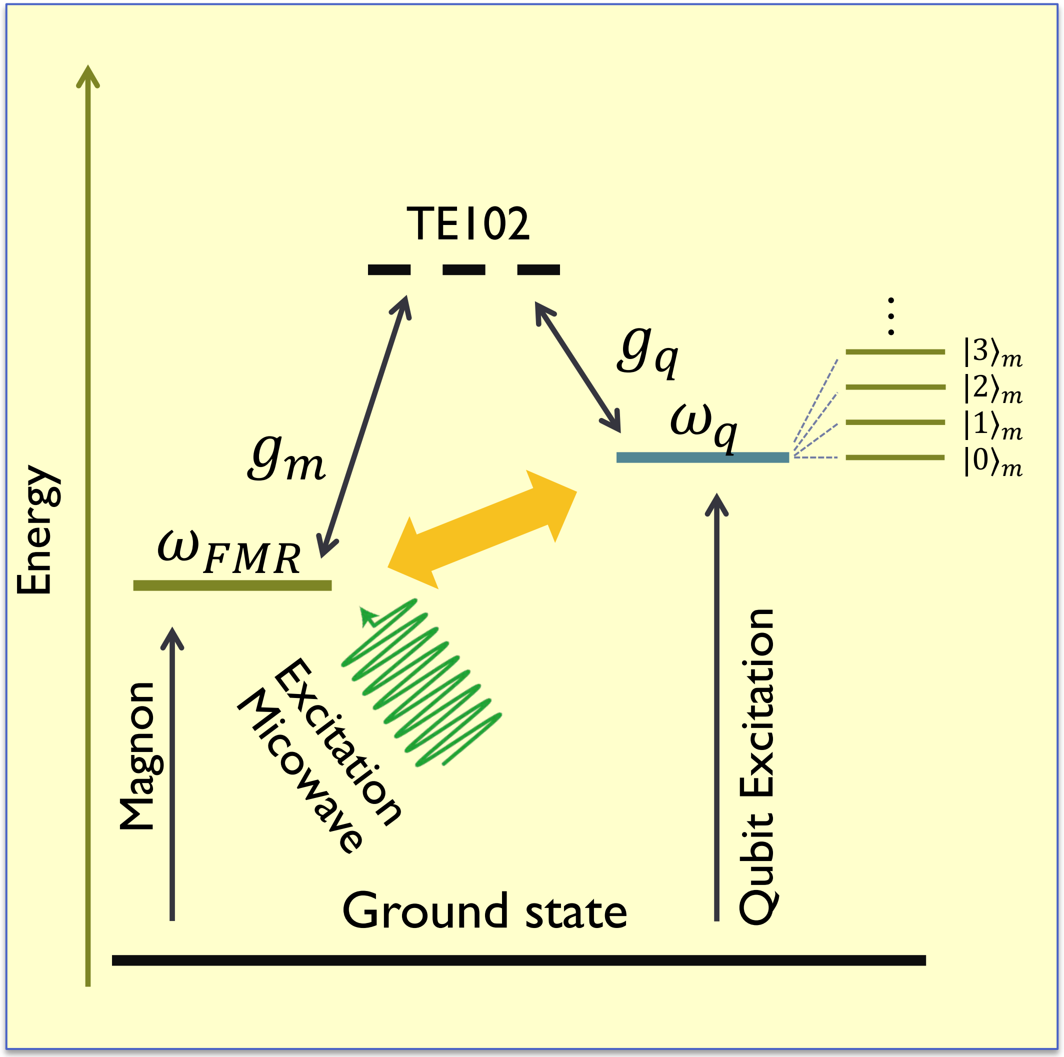

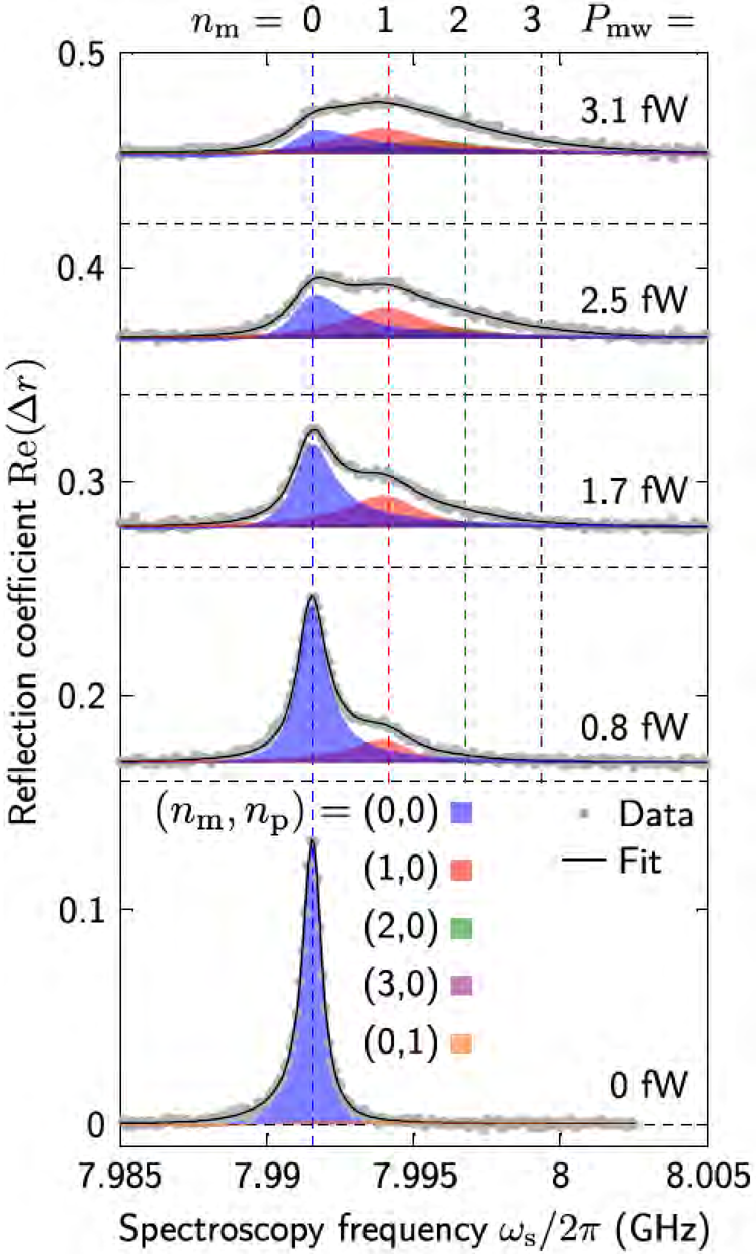

D. Lachance-Quirion et al. Sci. Adv. 3, e1603150 (2017).

Magnon-number-resolving spectroscopy

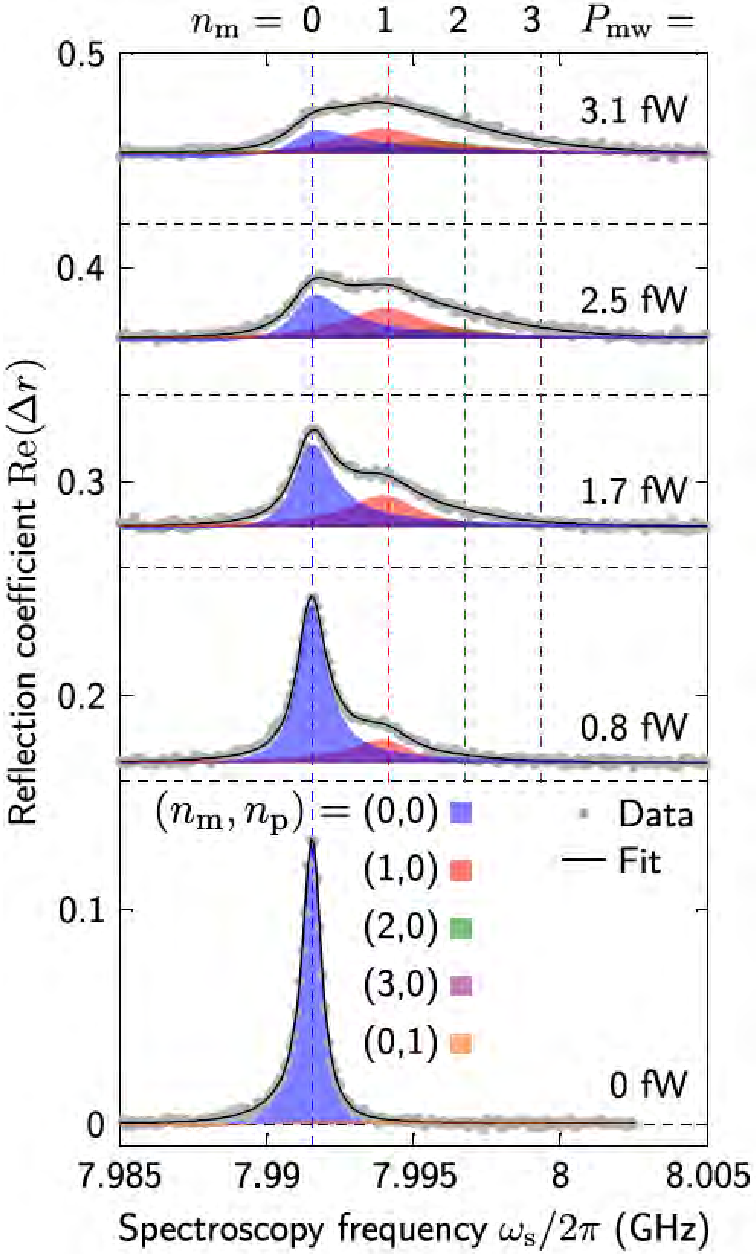

D. Lachance-Quirion et al.
Sci. Adv. 3, e1603150 (2017).

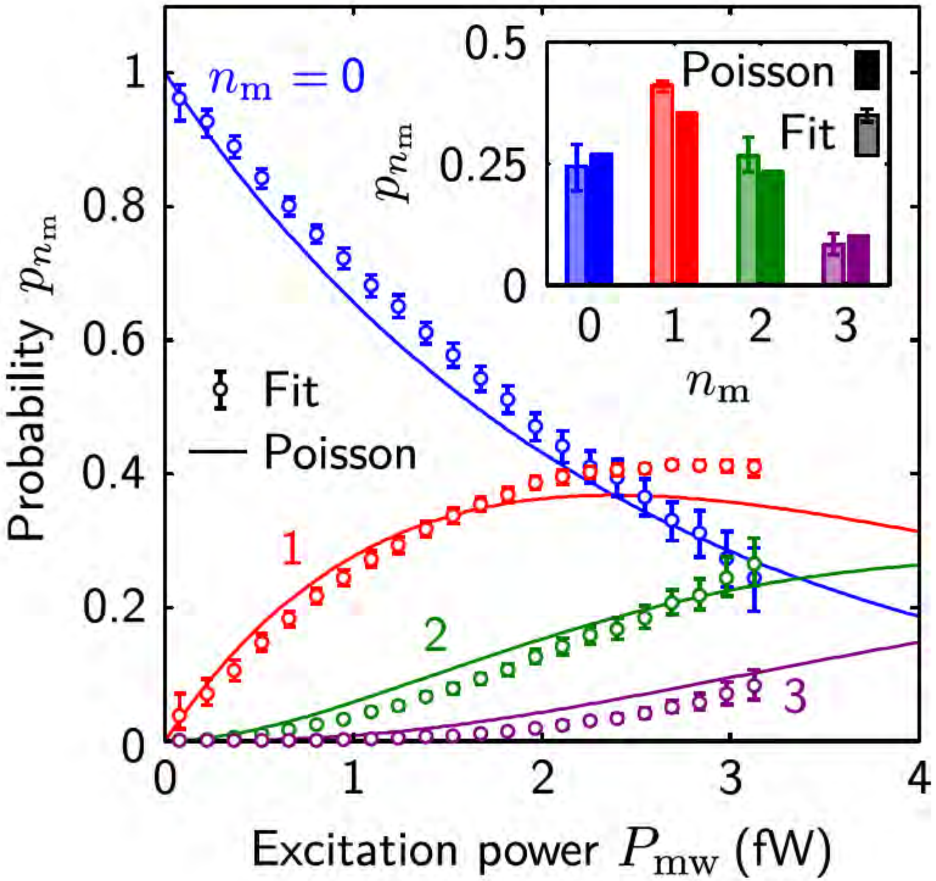

Model: J. Gambetta et al. Phys. Rev. A 74, 042318 (2006) Yale

Magnon number resolving via Ramsey interferometry

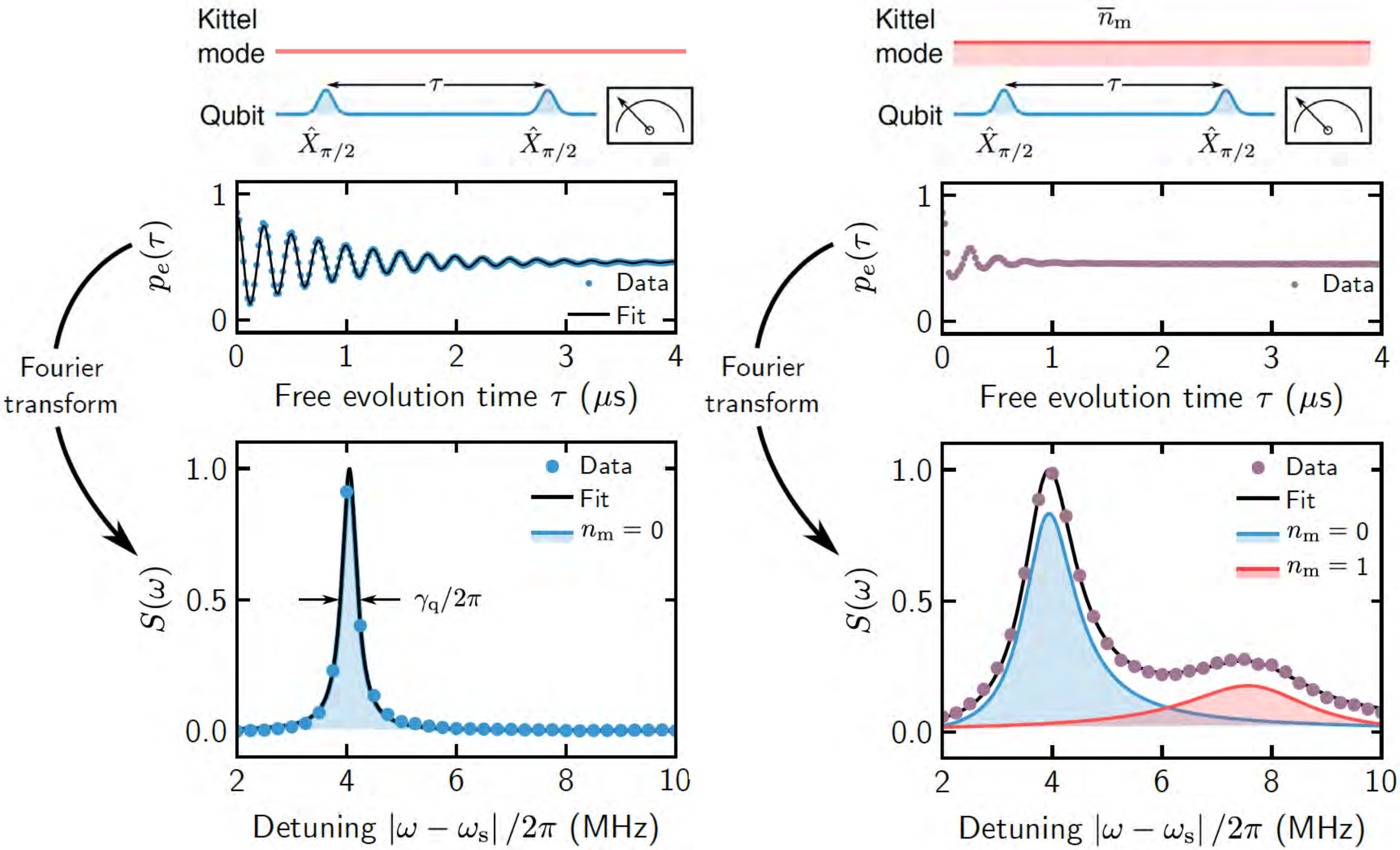

D. Lachance-Quirion et al. Applied Physics Express 12, 070101 (2019);
See also D. Lachance-Quirion et al. Sci. Adv. 3, e1603150 (2017)

Single-shot detection of a magnon

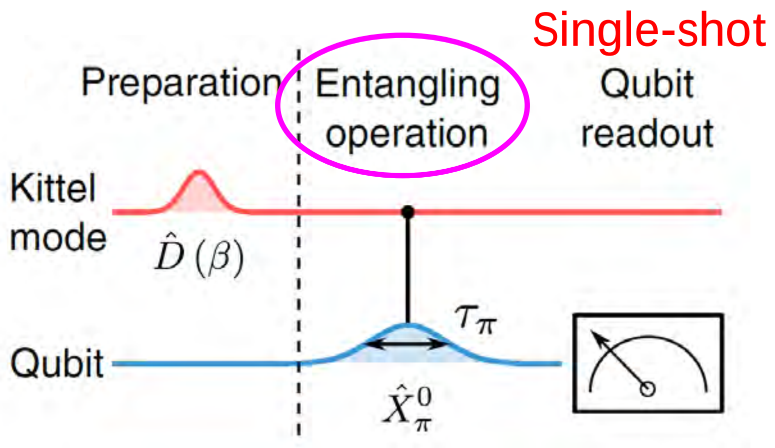

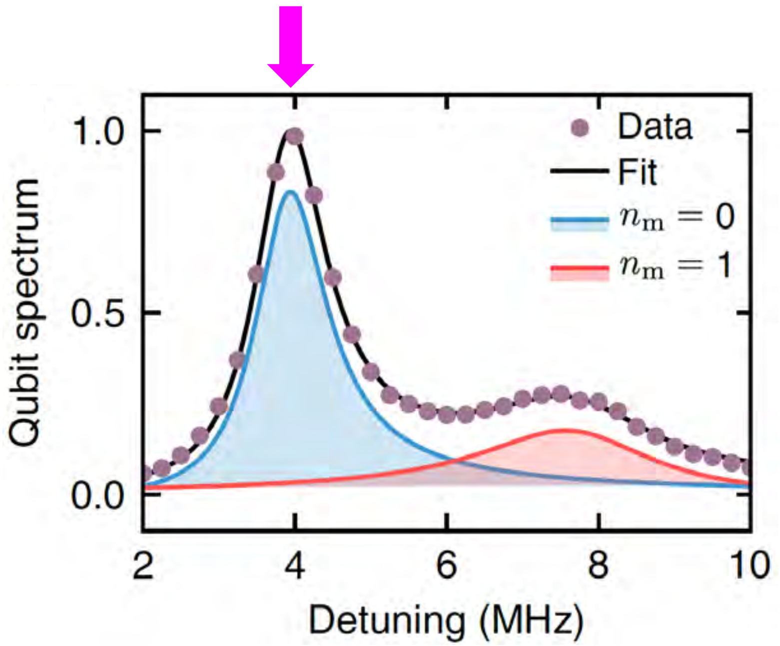

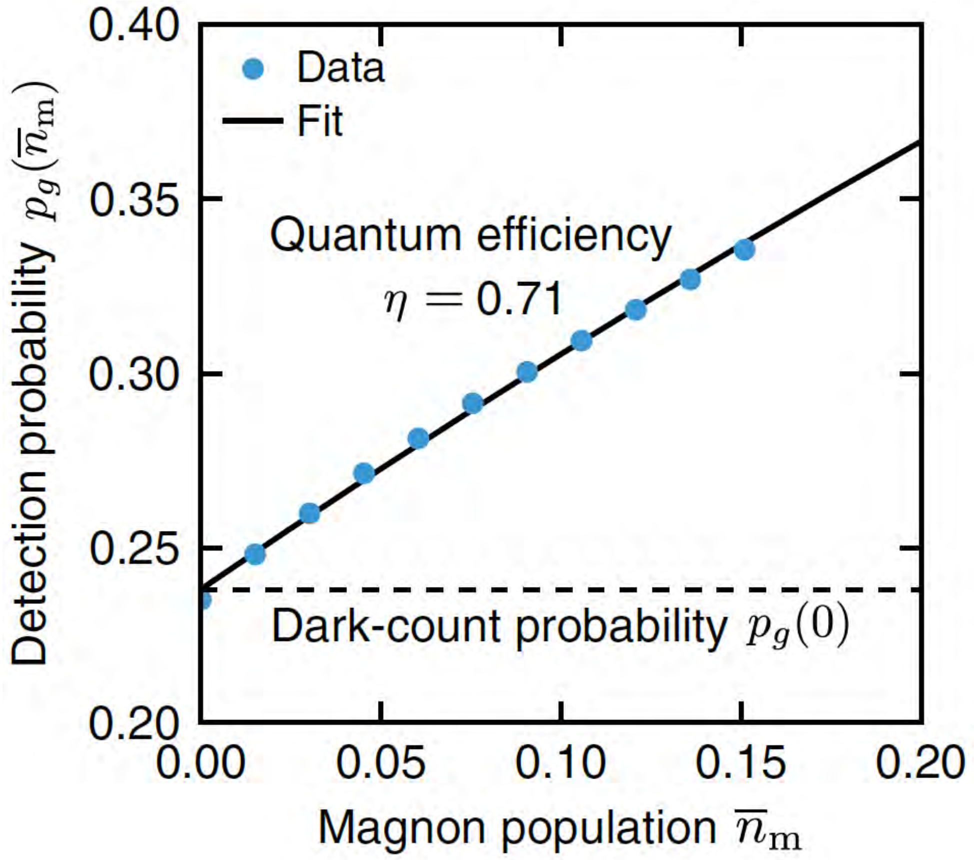

D. Lachance-Quirion et al. Science 367, 425 (2020)

Quantum electromechanics

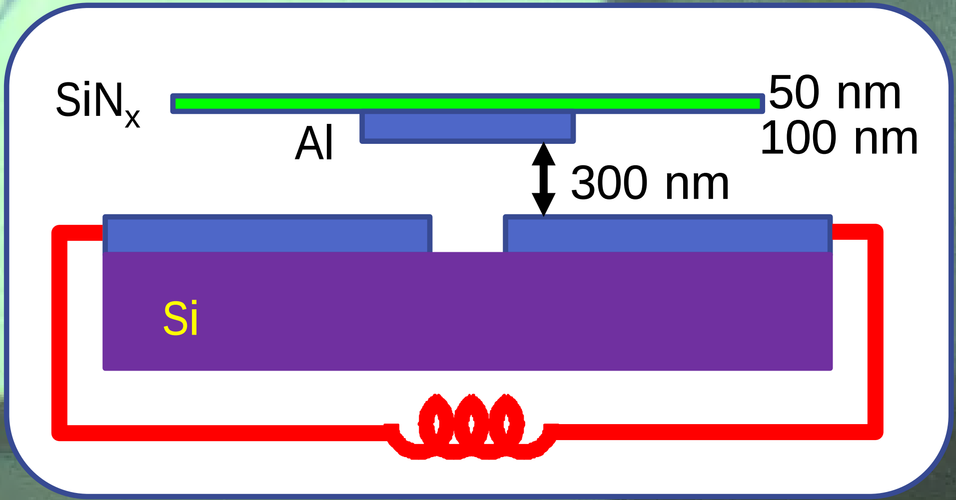

A. Noguchi et al. New J. Phys. 18, 103036 (2016)

Ground-state cooling

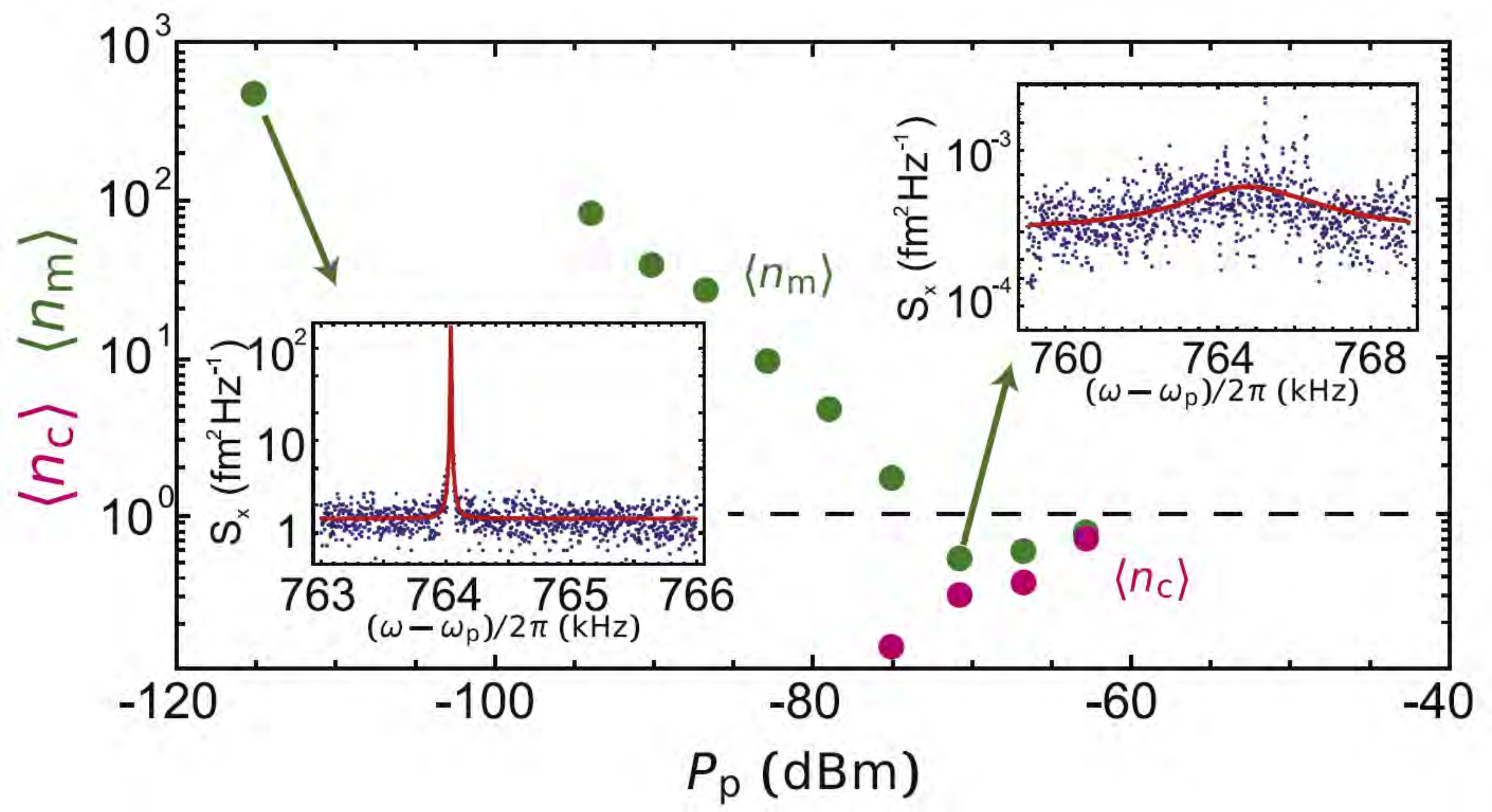

$$\langle n_m \rangle = 0.51 \pm 0.12$$

displacement ~ fm

A. Noguchi et al. New J. Phys. 18, 103036 (2016)

Summary

Superconducting qubits
= Nonlinear resonator circuits using Josephson effect
= Artificial atoms realized in electric circuits

- Superconducting quantum computing
    - High-fidelity control of a quantum system with a large Hilbert space
    - Challenges against decoherence, for scaling-up, and toward fault tolerance

- Microwave quantum optics
    - Circuit (cavity) QED & waveguide QED
    - Control and measurement of confined/itinerant microwave photons

- Hybrid quantum systems
    - Extending quantum technology to other degrees of freedom